GA–A24369

TARGET INJECTION AND TRACKING DEVELOPMENT IN SUPPORT OF NRL LASER-PLASMA PROGRAM ANNUAL REPORT TO THE U.S. DEPARTMENT OF NAVY

JANUARY 14, 2002 THROUGH MARCH 5, 2003

by
PROJECT STAFF

Work prepared under
U.S. Department of Navy
Naval Research Laboratory
Contract No. N00173-02-C-6007

DATE PUBLISHED: AUGUST 2003

GENERAL ATOMICS

DISCLAIMER

GA–A24369

TARGET INJECTION AND TRACKING DEVELOPMENT IN SUPPORT OF NRL LASER-PLASMA PROGRAM ANNUAL REPORT TO THE U.S. DEPARTMENT OF NAVY

JANUARY 14, 2002 THROUGH MARCH 5, 2003

by
PROJECT STAFF

Work prepared under
U.S. Department of Navy
Naval Research Laboratory
Contract No. N00173-02-C-6007

GENERAL ATOMICS PROJECT 39083
DATE PUBLISHED: AUGUST 2003

EXECUTIVE SUMMARY

Studies of laser-matter interactions require suitable targets as well as appropriate positioning of those targets. Key issues for the future of Inertial Fusion Energy (IFE) are the ability to manufacture large quantities of low-cost targets meeting precise specifications, the ability to inject (position) the targets accurately for laser shots, the ability to track the targets to predict their position in the chamber, and the survival of the target in a high-temperature reaction chamber before the shot. High-gain, direct drive targets have been proposed by the Naval Research Laboratory (NRL) for both the IFE and the Inertial Confinement Fusion (ICF) programs. The work this year has focused on developing the scientific basis for fabricating, characterizing, and injecting high-gain, direct-drive targets.

This report describes the work conducted this year for target injection and tracking. A companion report documents the work done for target fabrication and characterization development. Target injection research and development tasks included:

1. Modeling of target survival during injection.
2. Fabrication, software development, and initial testing of an experimental target injection and tracking system.
3. Development of an electromagnetic injection system as an advanced backup.
4. Support of Los Alamos National Laboratory (LANL) DT testing for targets.
5. Coordination of development to ensure target technologies are consistent.

In support of these tasks, our major accomplishments included:

1. Fabrication of all major components for single shot target injection and tracking.
2. Renovation of a building for inertial fusion energy target fabrication and injection studies (on internal funding).
3. Design, fabrication, and initial testing of a three-stage electromagnetic accelerator.
4. DT layering experiment in a torus with and without foams.
5. Extensive publications including target injection modeling and analyses of target survival as a function of chamber conditions.

Overall, the target injection workscope has significantly advanced the knowledge base in the area of inertial fusion target materials, target survival during injection, and target injection and tracking methodologies. The result of these tasks is a better understanding of the scientific basis for successfully injecting high-gain targets for a KrF laser inertial fusion system.

TABLE OF CONTENTS

LIST OF FIGURES

1. INTRODUCTION

At the heart of an Inertial Fusion Energy (IFE) power plant is a target that has been compressed and heated to fusion conditions by the energy input of the driver beams. For direct drive, the target consists of a spherical capsule that contains the DT fuel. The target must be accurately delivered to the target chamber center (CC) at a rate of about 5 to10 Hz, with a precisely predicted target location. The fragile targets must survive injection into the target chamber without damage. The NRL direct drive target consists of five layers: a central core containing DT vapor, a layer of solid DT fuel, a DT-filled CH foam ablator, an ~1 μm polymer seal, and an ~0.03 μm outer gold coating.

While IFE power plant design studies have suggested potentially plausible scenarios for both direct drive and indirect drive target injection, the purpose of the target injection and tracking development program is to provide the detailed scientific basis that will be necessary for fueling of future IFE power plants. This report describes the work done by General Atomics (GA) in the past year to assure that future target injection, and survival in the chamber, can be successfully accomplished.

2. KEY TECHNICAL ISSUES

The top-level critical issue for target injection and tracking is the ability to accurately and repeatedly place a target filled with DT ice at ~18.5 K, and meeting precise geometric requirements, at the center of a high-temperature target chamber at a rate of ~6 Hz.

Key issues associated with demonstrating a successful IFE target injection methodology are:

1. Ability of targets to withstand acceleration into chamber.
2. Ability of targets to survive chamber environment (heating due to radiation and gases).
3. Accuracy and repeatability of target injection.
4. Ability to accurately track targets.

3. LIST OF ACCOMPLISHMENTS

- We completed refurbishment of a large building (on internal funding) for Inertial Fusion Energy target injection and fabrication experiments.
- We fabricated and installed all major equipment for single shot testing with single axis tracking.
- We began operational firing of the target injection system.
- We developed software for control of the line scan camera frame grabbers for use with the QNX real time operating system.
- We performed stationary calibration of a target tracking detector (line-scan camera) achieving ±2.5 μm position-measurement repeatability.
- We performed calculations of the drag force and gas heat flux on a target for various distances between the target and a protective wake shield using DSMC.
- We designed and began testing a three-stage electromagnetic accelerator.
- We performed DT layering experiments achieving 1 μm RMS ice smoothness over foam in a torus.
- We calculated target heating with an external foam layer using temperature dependent thermal conductivity and heat capacity. We evaluated the possibility of allowing DT phase change during injection with at most very small vapor build up between the shell and DT.
- We attended technical meetings and prepared numerous publications as listed below in the publications and presentations section.

4. SUMMARY OF TASKS

4.1. TARGET SURVIVAL DURING INJECTION

Target survival during injection is a critical issue for IFE. The target must survive both the acceleration and the high temperature environment inside the reaction chamber.

We evaluated various in-chamber target protection schemes and conceived a new concept of protecting direct drive targets from heating with an outer membrane separated from the target through which laser beams would propagate. The membrane could be cooled with frozen gas that will evaporate in route to the target chamber.

We performed calculations of the drag force and gas heat flux on a target for various distances between the target and a protective wake shield using DSMC. These results were used to optimize the relative motion between a wake shield and target and to calculate the average heat flux around the target during injection with a shield.

Detailed analysis of convection heat transfer and gas condensation on direct drive targets was done to provide a more accurate estimate of the temperature rise. Careful examination of gas transport near the target surface indicates that shielding of the incident particle flux by uncondensed gas is important for pressures greater than 1 mTorr. Therefore, more accurate treatment of particle sticking must be used. High sticking coefficients will lower the allowable gas temperature and pressure in the chamber. The results for gas condensation heating are shown in Fig. 1. Transient analysis of the target thermal response was performed near the triple point using DT properties corresponding to each phase. The calculations provide better insight into the "knee" in the maximum temperature curve. As compared with previous estimates, lower allowable heat flux is predicted as the triple point is reached. For example (as shown in Fig. 2), for a 6 m radius chamber, target speed of 400 m/s, and initial target temperature of 18 K, just 0.6 W/cm^2 heat flux would cause the DT surface temperature to reach the triple point.

We calculated target heating with an external foam layer using temperature-dependent thermal conductivity and heat capacity. These calculations were carried out for a range of foam thicknesses and densities. An example result is that 130 μm of 0.25 g/cc foam is calculated to allow target survival with 2.2 W/cm^2 heat load for 15 ms. The thermal diffusivity of the foam does not change much with density because both the heat capacity and thermal conductivity increase proportionally. As the foam temperature increases, the heat capacity increases rapidly thereby decreasing the thermal diffusivity and improving target survivability. We started assessment of likely phase changes as the DT temperature exceeds the triple point. We checked the effect of lowering the initial target temperature to 16 K on

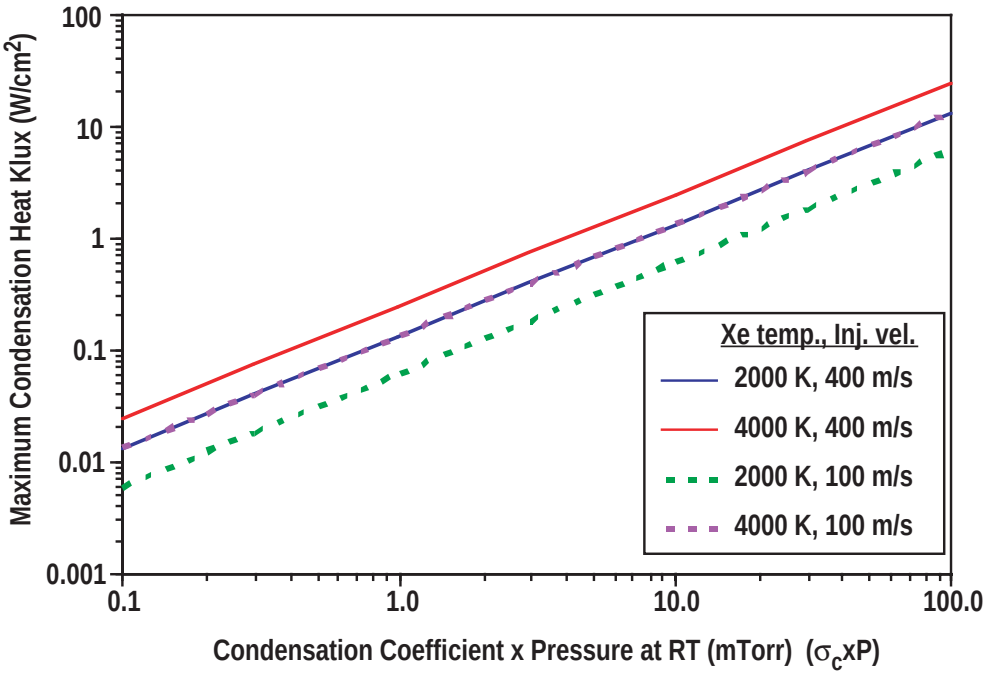

Fig. 1. Condensation heat flux versus condensation coefficient times pressure for various gas pressures and injection velocities.

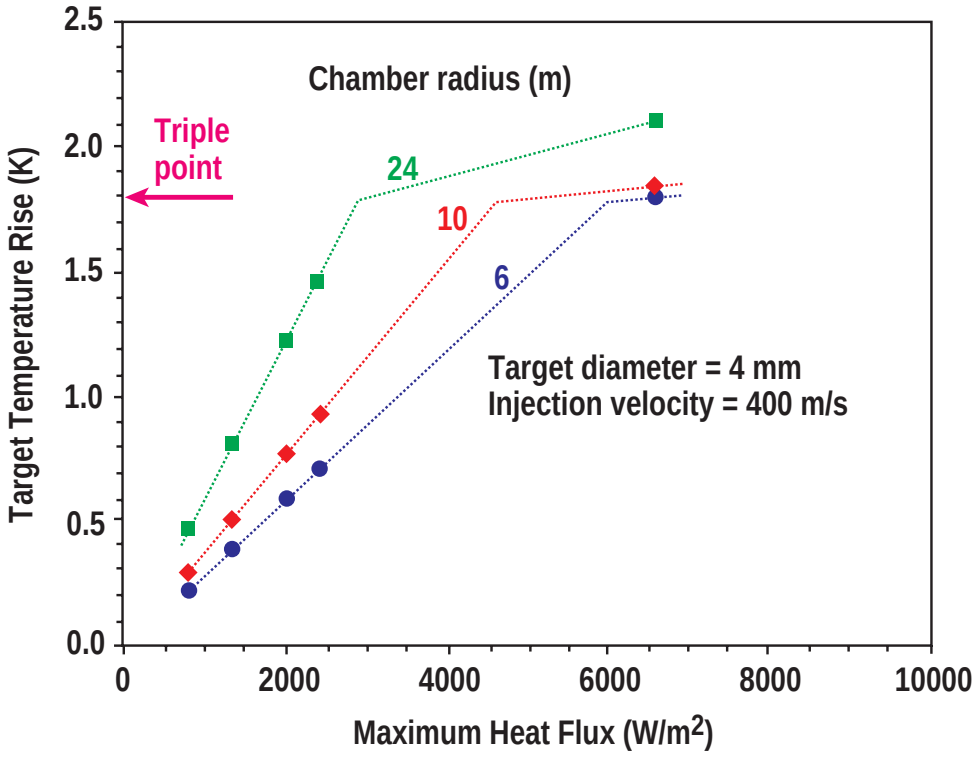

Fig. 2. DT target surface temperature rise versus heat flux for various chamber radii (assumes 18 K initial target temperature).

enhancing target survival (surface smoothness tests with reduced temperature are discussed below). This does help in increasing the thermal robustness of the target but is not sufficient. For example, for a 2.2 W/cm^2 heat flux, the time to reach the triple point is increased from about 2 ms for the 18 K case to about 5.2 ms for the 16 K case.

A target survival workshop was held on December 6, 2002 as part of the HAPL Project Review at NRL, Washington D.C. The goal of the workshop was to refine our understanding of direct drive target survival during injection and of constraints from the physics, fabrication and engineering communities — and decide what can be done to improve our position on this subject during the next three years. The format encouraged informal discussion guided and moderated by Dan Goodin and René Raffray. The following action items were identified:

1. NRL to evaluate the insulating foam target for stability (both uniformly dense and graded).
2. Schafer to look up the data on a "graded density" foams and see if this could be feasible.
3. NRL to confirm that a uniform DT vapor region thickness below the outer seal (of about 3 μm) is acceptable and, in the actual case of non-uniform heating, to provide guidance on how much variation is acceptable between the thickness of the vapor regions on opposite ends of the target (i.e., corresponding to the highest and lowest heat fluxes).
4. GA/UCSD to evaluate how much temperature drop there is to keep the insulated target cold (with beta decay heat) and determine how beneficial this temperature drop is with respect to survival estimates.
5. GA/UCSD to evaluate the effect of asymmetric heating in particular on local phase change behavior. A new multi-dimensional model being developed for the thermo-mechanical behavior of the target will help better understand this.
6. GA/UCSD to evaluate whether the insulated target with an outer seal that is permeable could actually be filled and "dryed" of DT in the outer foam.

We have completed an integrated multilayer radiation model including spherical and spectral integration. It will help determine the accuracy of previous reflectivity estimates using a simpler model and to determine the importance of volumetric heat generation as opposed to the previously considered surface heat flux approximation. We are completing the reflectivity calculations for Au and Pd coating on the target based on our integrated multilayer radiation model including spherical and spectral integration.

We are starting the development of the integrated target thermomechanics computer code. We are starting with a 1-D integrated model including the effect of evaporation and condensation in the gap between the DT/foam region and the GDP outer coat.

4.2. EXPERIMENTAL TARGET INJECTION AND TRACKING SYSTEM FABRICATION AND INITIAL TESTING

We renovated building 22 (on internal funding) for IFE target fabrication and injection research and development. A modular office building was also installed next to building 22. Figure 3 shows the building before and after renovation. Seismic calculations for installation of the injector line in building 22 were completed.

Fig. 3. The IFE target fabrication and injection facility before and after renovation.

The target injection and tracking system is required to inject targets at high velocity (~400 m/s), position them to within ±5 mm, and demonstrate tracking the targets to allow alignment of the laser beam with the target centerline to ±20 μm. A light gas gun was selected for the acceleration because of its simple, low-cost technology. The system consists of a fast gas control valve, a target-loading revolver, an 8-m gun barrel, a gas removal system, a sabot removal system, and optical tracking devices with real-time position prediction functionality. All of these components were fabricated and installed this year. Photographs of these items are shown in Fig. 4. The revolver and gun barrel arrived much later than expected due to fabrication problems. The gun barrel was received in November, but was about 0.001 in. undersized in i.d. at the section joints due to shrinkage during heat treatment (after the plating process for the Morse Tapers). This was corrected by a local vendor. The revolver chamber was not received until January 2003.

Propellant valve power supply

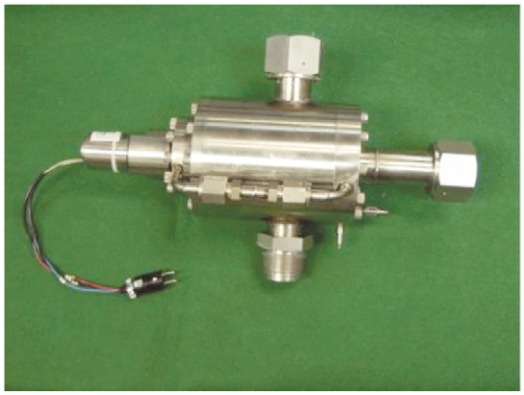

Propellant valve

Revolver chamber

Gun barrel

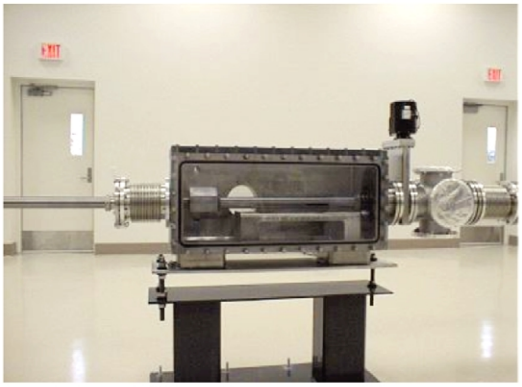

Gas divertor chamber

Fig. 4. Major target injection and tracking system components. (Part 1 of 2.)

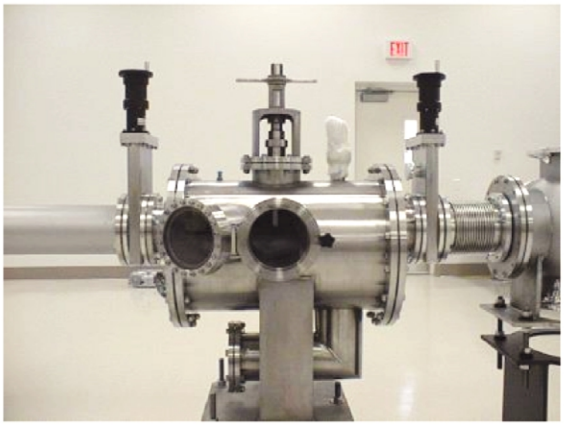

Sabot deflector

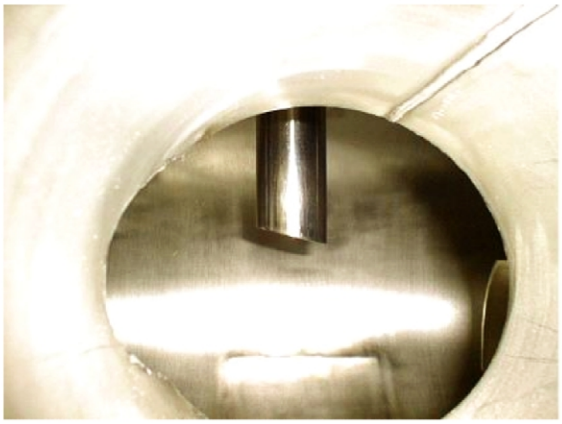

Sabot deflector closeup

Sabot deflector with camera and high intensity lighting

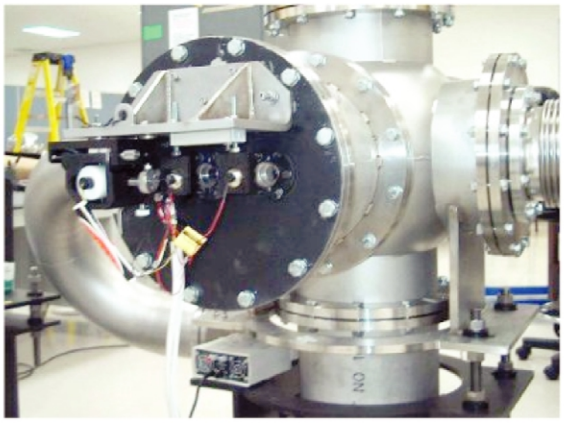

Tracking system lasers

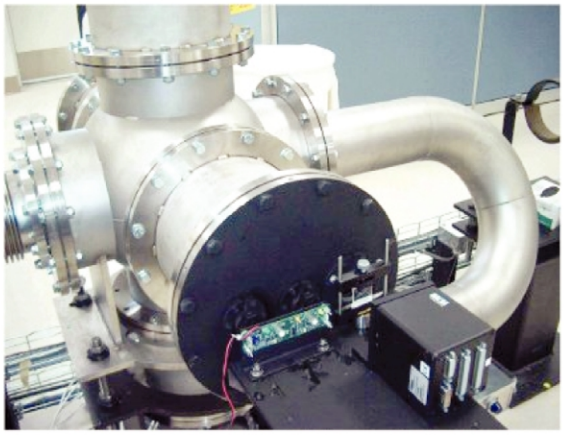

Tracking photodiodes and line scan camera

Fig. 4. Major target injection and tracking system components. (Part 2 of 2.)

We assembled the Opto22 control cabinet. We prepared a simulation program to facilitate the programming and testing of the overall injection system control software that communicates with the "fast" portions of the tracking system. We began detailed programming of the Opto22 systems for overall system control. We developed a communication protocol between the main revolver system drive motor controller and the Opto22 units and developed basic motor instruction programs for the revolver. Initial installation of the OPTO22 system is complete, including running of power and data cables. All sensors and equipment controlled by OPTO22 have been preliminarily installed and connected. The revolver motor and fast acting propellant valve were tested with the Opto 22 control system.

The lab computer running LabVIEW software/hardware is being set up to take and record traces for the operation of the fast acting valve system and of the gun barrel pressure transducers.

We completed the Hazardous Work Authorization for the entire injection and tracking system. We developed safe operating protocols for the laser tracking systems during alignment and maintenance (with the protective covers removed).

The revolver assembly was delivered in January. This was the last major equipment component required for single shot testing. We ordered the remaining tracking items to complete three detectors. We degreased and deburred the gun barrel i.d. — especially around the pressure sensor ports. We set up and leveled the gun barrel in its stands, connected it to the muzzle and muzzle box, and manually pushed one piece sabots through the barrel to find the smallest i.d. We completed modifications to sabot deflector assembly (added a light port and port window shields).

We obtained a supply of sabots for sabot separation testing. First sabot shots through the revolver, 8 m barrel, muzzle box, sabot separation chamber, and target catcher were performed. We completed modification of an earlier target-tracking device and installed it into the injector at the end of the gun barrel for use in sabot separation detection. We identified and purchased new lights, along with lenses, that allow the fast camera to be used for recording injector shots. High-speed video shots of sabots in motion up to 300 m/s were recorded with and without the sabot deflector in place.

4.3. ELECTROMAGNETIC INJECTOR

A repulsive type electromagnetic accelerator has the potential of providing highly repeatable shots of sabots carrying cryogenic targets. The magnetic approach also offers the ability to decelerate the sabot after reaching the required velocity. This could be used to separate it from the target and then deflect it for reuse or recycling. The technical approach developed for accelerating the sabot is a linear induction motor, which uses an aluminum ring (sabot) as the armature. This concept uses a series of small coils, each powered by a

charged capacitor. Energy is released from the capacitor by a thyristor at the instant the sabot is optimally positioned to take advantage of the coil's radial magnetic field, which accelerates it axially. As the capacitor discharges through the coil, one complete (or one-half) sine wave cycle occurs in both the coil and the aluminum sabot by induction while the sabot moves through the spacing between coils.

Much of the EM injector work was accomplished by Poweron Inc. under subcontract to GA. We developed a preliminary baseline configuration for a 16 to 20 stage 100 m/s electromagnetic injector. We developed a design concept for individual stages including coil and power circuit configuration. We prepared generic stage engineering layout and engineering sketches for mechanical components and initiated design of a fiber optic position sensing system including photodiode electronics. Injector design drawings and sketches are attached in Appendix A.

We held an injector review teleconference to address issues that have been raised with the use of electromagnetic injector concept for target acceleration. We investigated methods to lower the peak acceleration and revised the baseline concept from a full sine wave per stage to half sine. This lowered the peak to average acceleration from about 3.5 to 2. We developed and demonstrated a fiber optic position sensor circuitry using super bright LED's, 1 mm plastic fiber and photodetectors, and developed and tested prototype thyristor gate drive circuitry.

We completed mechanical fabrication and assembly of the injector support and the high voltage, low voltage, and timing/driver control panel. Low resistivity sabots were fabricated from high purity aluminum. We conducted initial tests with the first stage of the injector and all systems functioned as anticipated.

We completed fabrication of Stage 2 and Stage 3 coils, high voltage mechanical and electrical assemblies, driver/timing electronics circuit board, and sensor electronics (photograph in Fig. 5). We completed assembly and check out of all injector high voltage/high current hardware. We completed assembly and checkout of all fiber optic sensor and trigger electronics.

Initial tests of firing sabots with multiple stages resulted in the sabots getting caught between stages. We are now working to achieve a stable transition between stages during acceleration. We developed two different magnetic profiles of the sabot in the coils to determine the causes of instability and found that axial magnetic field curvature reverses as the sabot passes out of the primary coil, causing instability. We fabricated and installed a glass guide tube and successfully fired the first stage. The sabot seemed to smoothly exit the glass tube.

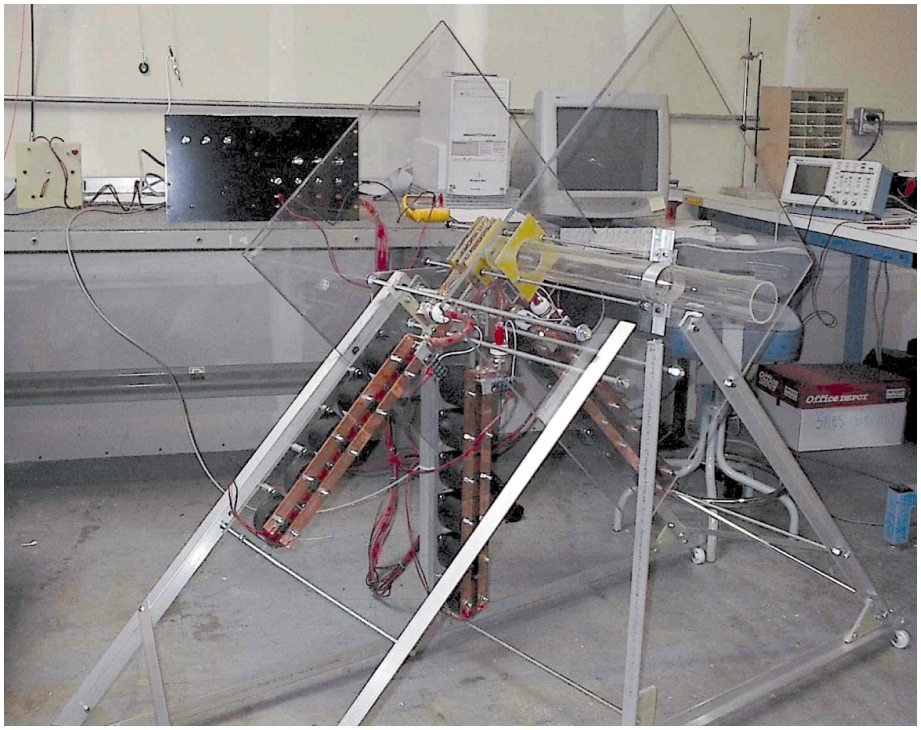

Fig. 5. Three-stage electromagnetic injector.

4.4. TRACKING SYSTEM

Much of the tracking system work was accomplished by Anderson Engineering under subcontract to GA. We completed the target tracking Software Design Specification and prepared the Software Test Plan. Software is tested at the unit, module, and system levels. Unit and module testing use “White Box” and “Black Box” methods to develop test cases.

We developed a protocol for communication between the TPPS and the target injection control computer. The protocol uses TCP/IP communication and is similar to the FTP protocol. We started writing and testing TPPS software with the initial code being for control of the line scan camera and framegrabber.

The line forming laser diodes that we use for target position detection are not very uniform across the beam. Additionally, the initial position detection tests showed a significant amount of constructive and destructive interference of the laser illumination. The result is “ringing” at the edges of the target shadow. We procured a diffuser and laser diode module to test for improved target position detection. The diffuser is designed to reduce the level of coherence of the illumination. Reducing the coherence will reduce the levels of interference. We selected a narrow elliptical diffuser and, therefore, used a beam forming laser instead of a line forming laser to produce the needed “curtain” of light. The diffuser did not improve the situation but caused large variations in beam intensity over short scale lengths.

We mounted the target tracking laser, line-scan camera, and optics in a Target Position Detector assembly and conducted testing of the laser-based tracking system with positioning of a stationary target using translators. The illumination was guided through the windows of the vacuum chamber. A three-axis translation stage was mounted onto the equipment to allow the target to be precisely located. Test results showed a 3.5 μm variation of position without moving the target. When the target was moved away and returned to the same location, position results were reproducible to about 8 μm on these first attempts. Using an improved algorithm, when the target was moved away and returned to the same location, the position measurement results were reproducible to ±2.5 μm. The position measurement results are not quite linear. Over a range of 8 mm in target position, the position error from a least squares fit straight line was ±31 μm. We performed additional tracking system testing over a range of 1 mm and found the position error from an end point fit straight line is ±10 μm.

We performed testing with the LED illumination boards and the photodiode boards for tracking timing. We observed that the light emanating from the LED was not uniform in the near field. By adjusting the collimating lens, we were able to create an image of the emitting element of the LED. Also, the LED light appeared to be reflected internal to the LED, so the LED did not look much like a point source. As a consequence, the light that was collimated from the LED was not adequate to allow the photodiode to detect a target at a distance of 1 m. We increased the sensitivity of the target timing sensor boards and identified a low power laser illumination that is capable of providing adequate illumination. The use of a 0.7 deg line generating lens produces the required illumination at the detector. We completed testing of the revised photodetector board with the laser illumination. The higher illumination level and more effective collimation of the laser compared to the LED and the increased gain of the photodetector board allowed the board to detect plastic spheres in flight.

We completed integration testing of the multifunction data acquisition board. This board receives trigger and up/down signals from the photodetector board, predicts the time when the target will be in the field of view of the line scan camera, and generates trigger signals to the camera. We used the discrete I/O capability of the multifunction board to simulate the photodetector board signals in order to measure the timing using an oscilloscope.

We developed a QNX driver for the Epix framegrabber and the Dalsa line scan camera. The driver allows the software to set up the camera to take an image and to store the image. We discovered that the Dalsa camera must operate at a minimum frame rate and modified the software to cause the camera to operate continuously prior to target arrival. We will begin to incorporate this detector into operational shot testing.

4.5. SOLID DT LAYERS IN FOAM

The DT work was done at LANL with participation from GA. The emphasis was on layering DT in a torus and measuring the layer smoothness. Initially, the layers were made without foam and later with foam. A brief summary of the work is given here. A more detailed description is given in Appendix B, "Studies of Solid DT Layers in Foam."

The affect of DT aging on DT ice surface smoothness was measured early in the year. The DT was layered in a Beryllium torus. Surface smoothness remained nearly constant at less than 2 μm RMS for 32 days and then started increasing about 0.1 μm per day thereafter for 10 days.

We then obtained a 2 mm inner diameter torus and covered it with a 74 μm thick foam layer. Liquid DT was added to the torus to fully fill the foam and provide an additional pure DT layer. Beta layering was then allowed to occur and surface smoothness measured. The foam layer gradually decreased over several weeks (and many experiments) from 74 μm to about 43 μm.

Although the foam layers are quite rough, the DT layer assumes a smooth shape above the foam. The DT was about twice as smooth (approximately 1 μm RMS) above the foam as it had been in previous experiments without foam. We believe this is likely because the fine cell structure of the foam causes freezing to begin with the formation of many small randomly oriented crystallites. These crystallites should propagate into the pure DT solid layer, reducing the tendency to form large crystalline facets at the solid-vapor boundary. Also, the foam provides large numbers of nucleation sites so the liquid does not supercool prior to freezing.

There is a possible detrimental affect of having foam in the targets. DT voids in the foam cells may become trapped and not able to migrate to the target center.

Cooling the targets from 19.25 to 15 K resulted in 50% to 75% increases in surface roughness. Warming back up to 19.25 K only improved surface smoothness by about 15%.

4.6. COORDINATE TASKS WITH OTHER IFE COMPONENTS

This task is to coordinate target activities and participate in Laser IFE community workshops to ensure technologies pursued are consistent with the overall IFE systems development. We hosted the 4th Laser IFE Program Workshop on April 4–5, 2002. Our publications and workshop presentations are noted below. Many of the meeting presentations are currently archived on the ARIES website at http://aries.ucsd.edu.

5. FY02 PUBLICATIONS

Petzoldt, R.W., D.T. Goodin, A. Nikroo, E. Stephens, N. Siegel, N.B. Alexander, A.R. Raffray, T.K. Mau, M. Tillack, F. Najmabadi, S.I. Krasheninnikov, and R. Gallix, "Direct Drive Target Survival during Injection in an Inertial Fusion Energy Power Plant," Nucl. Fusion, **42**, 1351 (2002).

Goodin, D.T., A. Nobile, J. Hoffer, A. Nikroo, G.E. Besenbruch, L.C. Brown, J.L. Maxwell, W.R. Meier, T. Norimatsu, J. Pulsifer, W.S. Rickman, W. Steckle, E.H. Stephens, and M. Tillack, "Addressing the Issues of Target Fabrication and Injection for Inertial Fusion Energy," Proc. 22nd Symp. on Fusion Technology, Helsinki, Finland, 2002, to be published in Fusion Engineering and Design.

Mikhail L. Shmatov, Ronald W. Petzoldt, and Emanuil I. Valmianski, "Measures to Provide Survival of the Direct Drive and Fast Ignition, Direct Compression Targets in the Reaction Chamber," Fusion Technology **43**, No. 3 (2003).

Emanuil I. Valmianski, Ronald W. Petzoldt, and Neil B. Alexander, "Wake Shield Target Protection," Fusion Technology **43**, No. 3 (2003).

Elizabeth H. Stephens, Abbas Nikroo, Daniel T. Goodin, and Ronald W. Petzoldt, "Optimizing High-Z Coatings for Inertial Fusion Energy Shells," Fusion Technology **43**, No. 3 (2003).

A.R. Raffray, R. Petzoldt, J. Pulsifer, M.S. Tillack, and X. Wang, "Thermal Behavior and Operating Requirements of the IFE Direct-Drive Target," To be published in Fusion Technology.

5.1. PRESENTATIONS AT THE 2ND IAEA TECHNICAL MEETING ON THE PHYSICS AND TECHNOLOGY OF IFE TARGETS AND CHAMBERS AT GENERAL ATOMICS 17-19 JUNE 2002.

E. Valmianski, "Wake Shields for Protection of IFE Targets during Injection."

R. Petzoldt, "Experimental Target Injection and Tracking System."

E. Stephens, "Palladium and Palladium Gold Alloys as High Z Coating for IFE Targets."

Greenwood, "Thickness and Uniformity Measurements of Thin Sputtered Gold Layers on ICF Capsules."

5.2. LASER IFE PROGRAM REVIEWS

- April 2002
  - — D. Goodin, GA Target Fabrication Tasks
  - — E. Stephens, Coating Development
  - — R. Petzoldt, Status of Target Injection and Tracking
- December 2002
  - — D. Goodin, Target Fabrication/Injection Plan plus GA Target Fabrication Effort
  - — R. Petzoldt, Status of Target Injector, In-Chamber Tracking
  - — R. Raffray, Target Survival Calculations
  - — R. Raffray and D. Goodin, Target Survival Workshop

5.3. OTHER

- 22nd Symp. on Fusion Technology, Helsinki, Finland, D. Goodin, “Addressing the Issues of Target Fabrication and Injection for Inertial Fusion Energy.”
- Snowmass 2002 Fusion Energy Sciences Summer Study
  - — R. Petzoldt, “Membrane Support of Targets.”
  - — J. Dahlburg, “Status of Target Fabrication and Injection.”
- Numerous presentations at ARIES meetings

6. ACKNOWLEDGMENT

This report was prepared for the U.S. Department of Navy, Naval Research Laboratory Contract No. N00173-02-C-6007.

APPENDIX A
ELECTROMAGNETIC INJECTOR DESIGN DRAWINGS AND SKETCHES

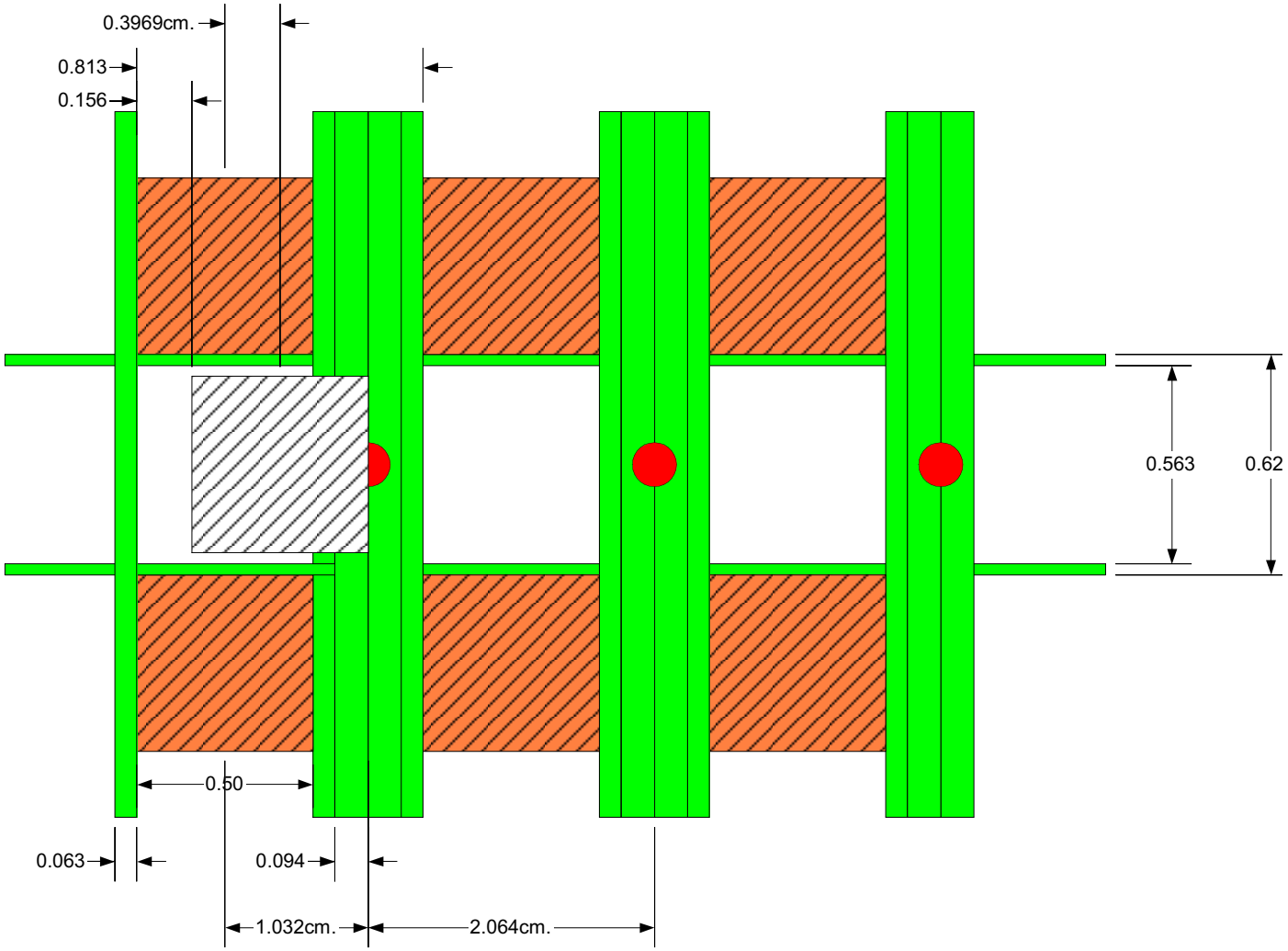

POWERON
1185 Park Center Dr. Ste S
Vista, CA 92083
760-599-0440
760-599-0404 (fax)

POWERON

CONFIGURATION

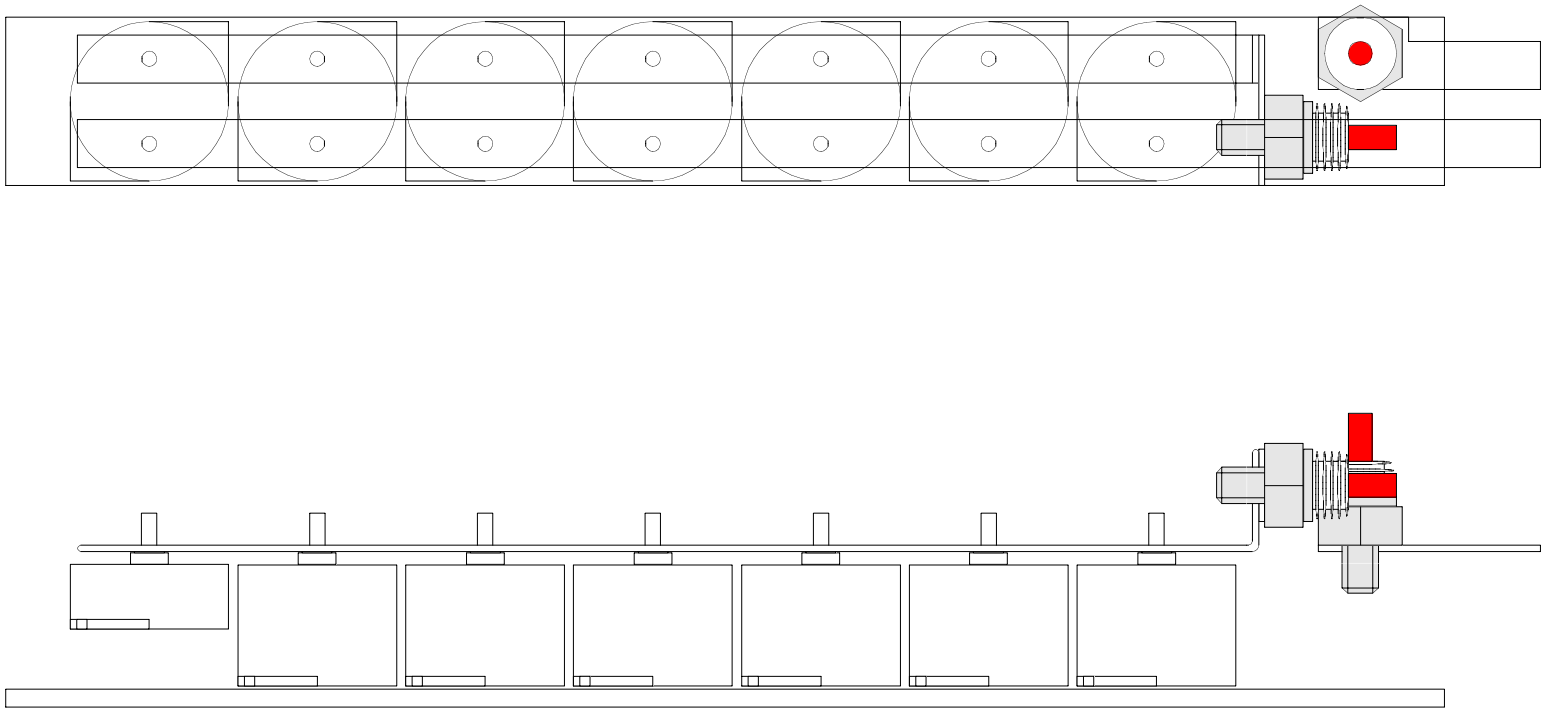

POWERON
1185 Park Center Dr. Ste S
Vista, CA 92083
760-599-0440
760-599-0404 (fax)

POWERON

BUS LAYOUT

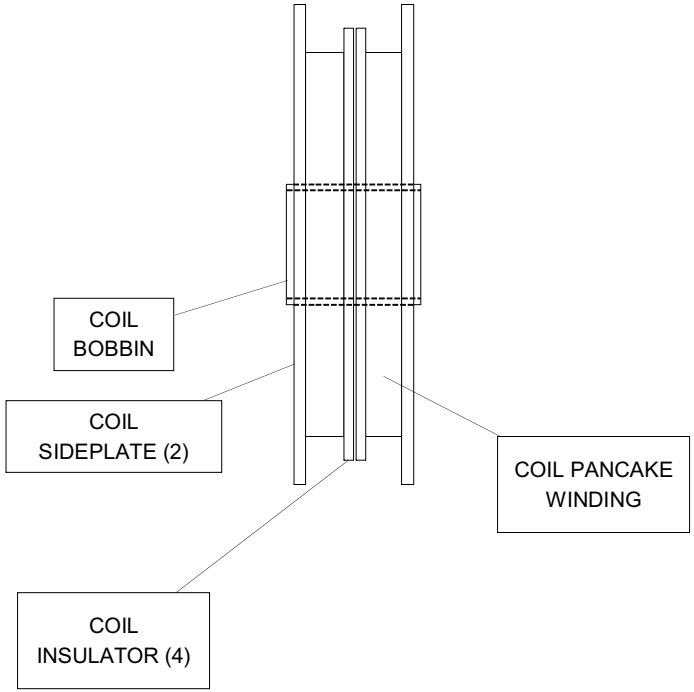

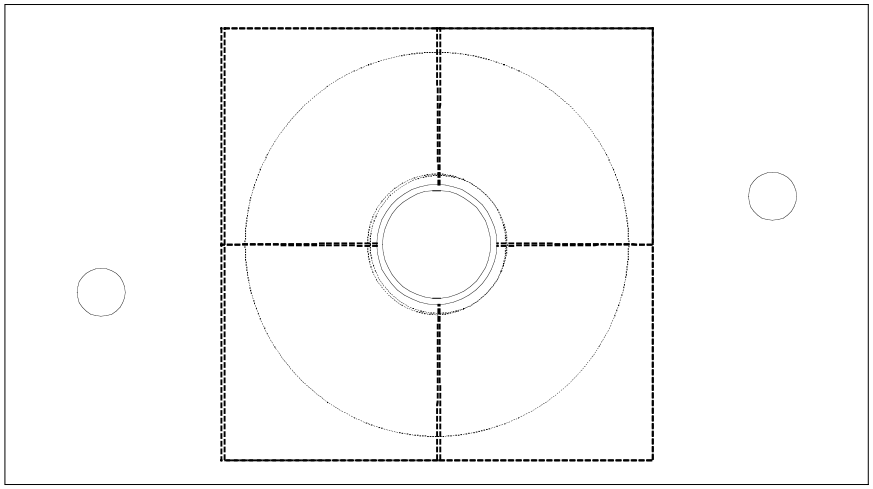

POWERON
1185 Park Center Dr. Ste S
Vista, CA 92083
760-599-0440
760-599-0404 (fax)

POWERON

COIL ASSY

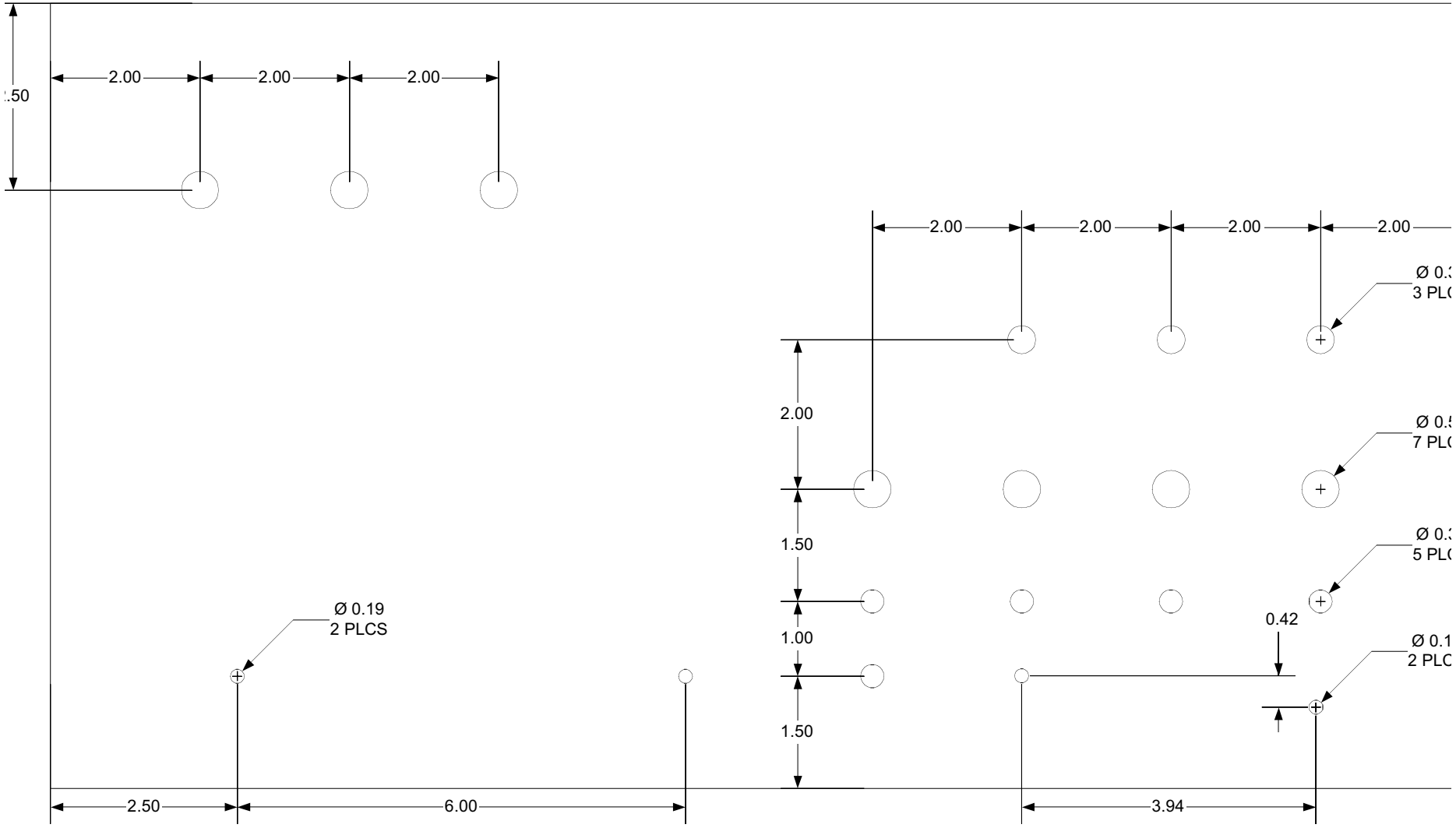

Notes

1. Remove all burrs and round sharp corners.

2. Make from 0.125 in thick

POWERON
1185 Park Center Dr. Ste S
Vista, CA 92083
760-599-0440
760-599-0404 (fax)

POWERON

CONTROL PANEL

SIZE	FSCM NO	DWG NO

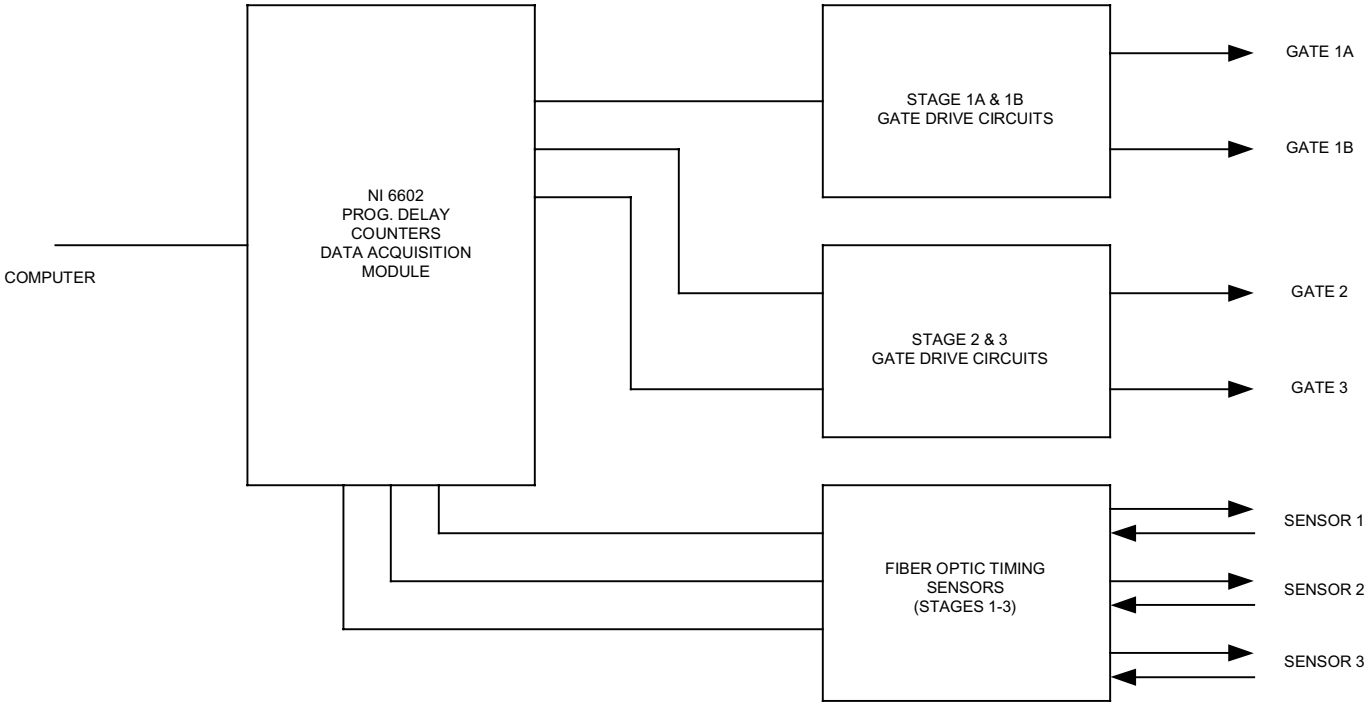

POWERON
1185 Park Center Dr. Ste S
Vista, CA 92083
760-599-0440
760-599-0404 (fax)

POWERON

INJECTOR BLOCK DIAGRAM

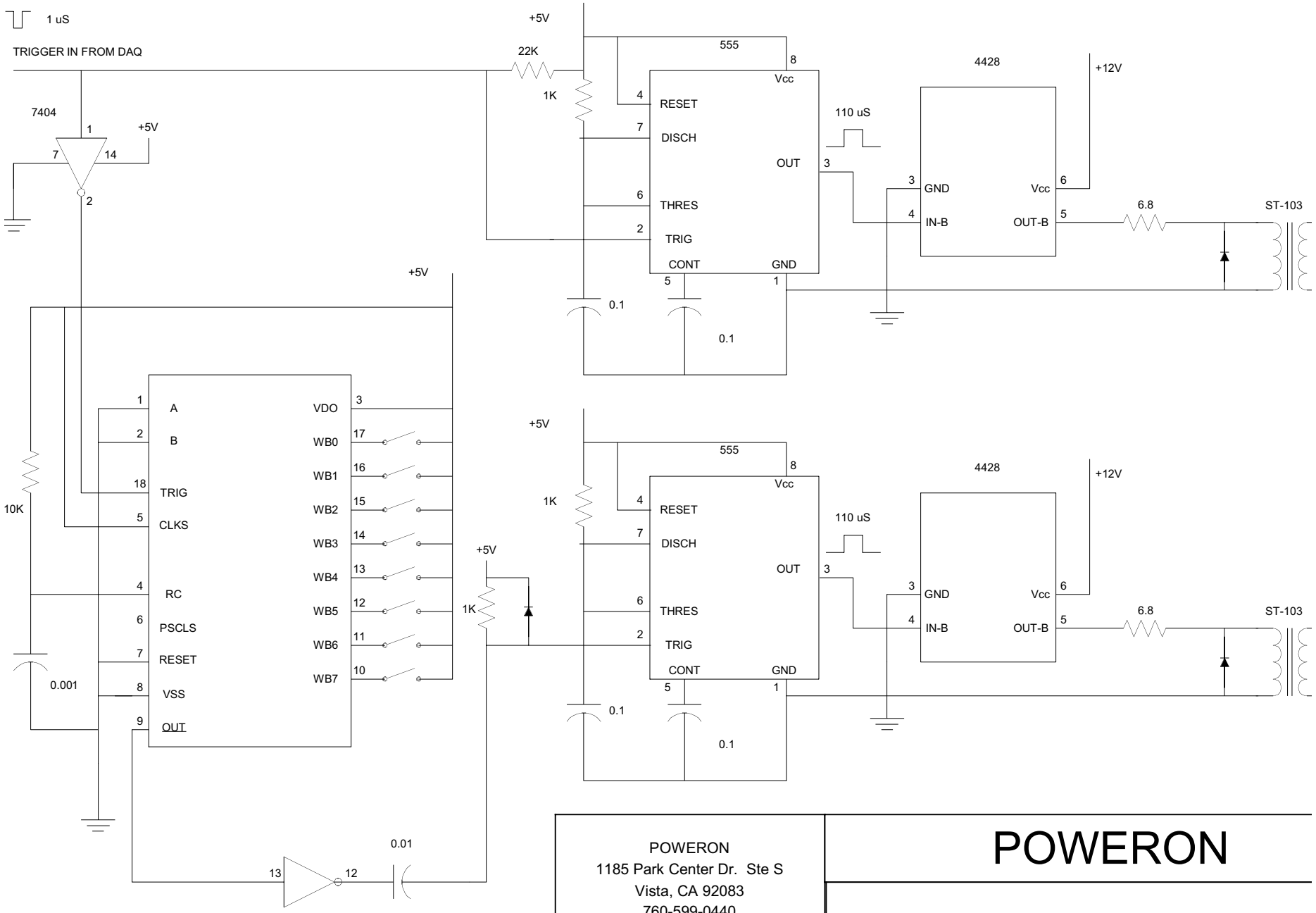

POWERON
1185 Park Center Dr. Ste S
Vista, CA 92083
760-599-0440
760-599-0404 (fax)

POWERON

GATE DRIVE 1A & 1B CIRCUIT BOA

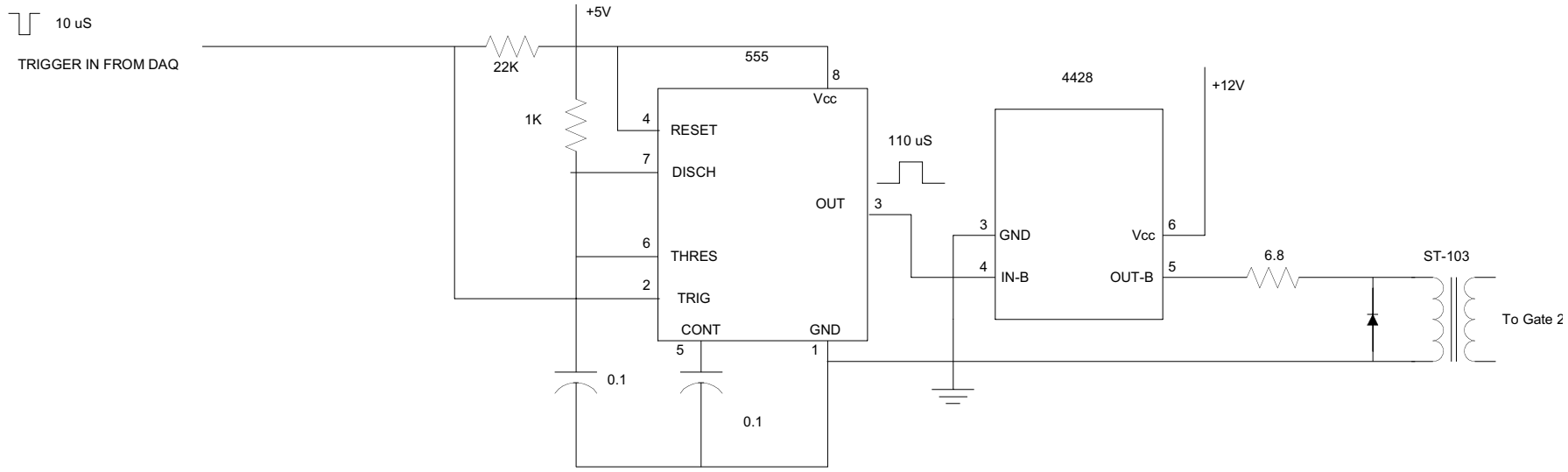

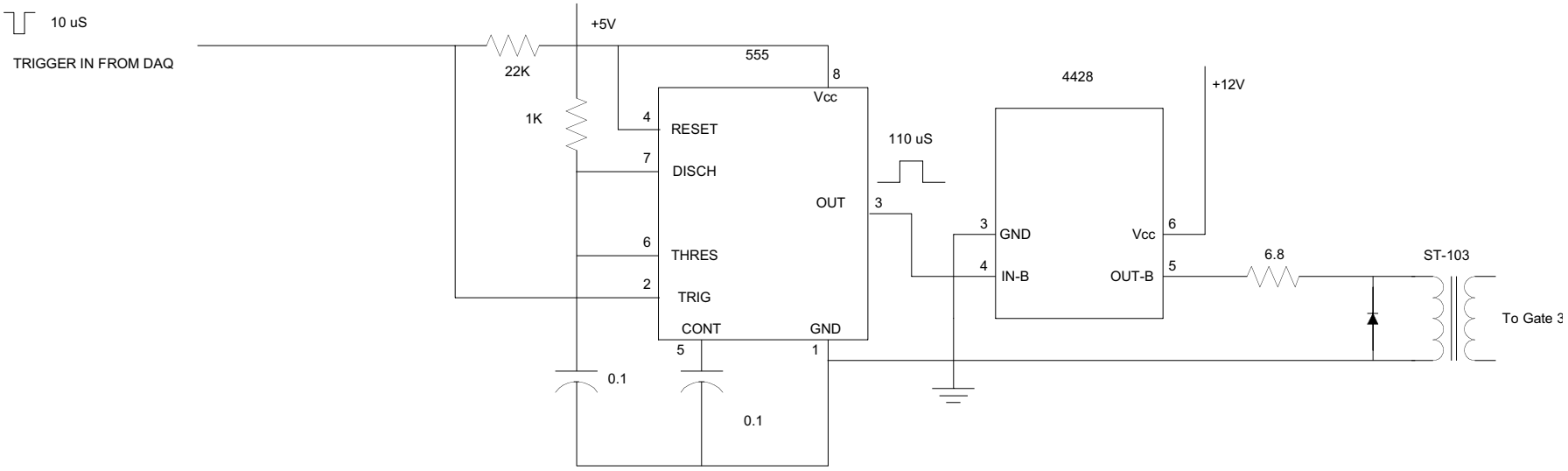

POWERON
1185 Park Center Dr. Ste S
Vista, CA 92083
760-599-0440
760-599-0404 (fax)

POWERON

GATE DRIVE 2 & 3 CIRCUIT BOAR

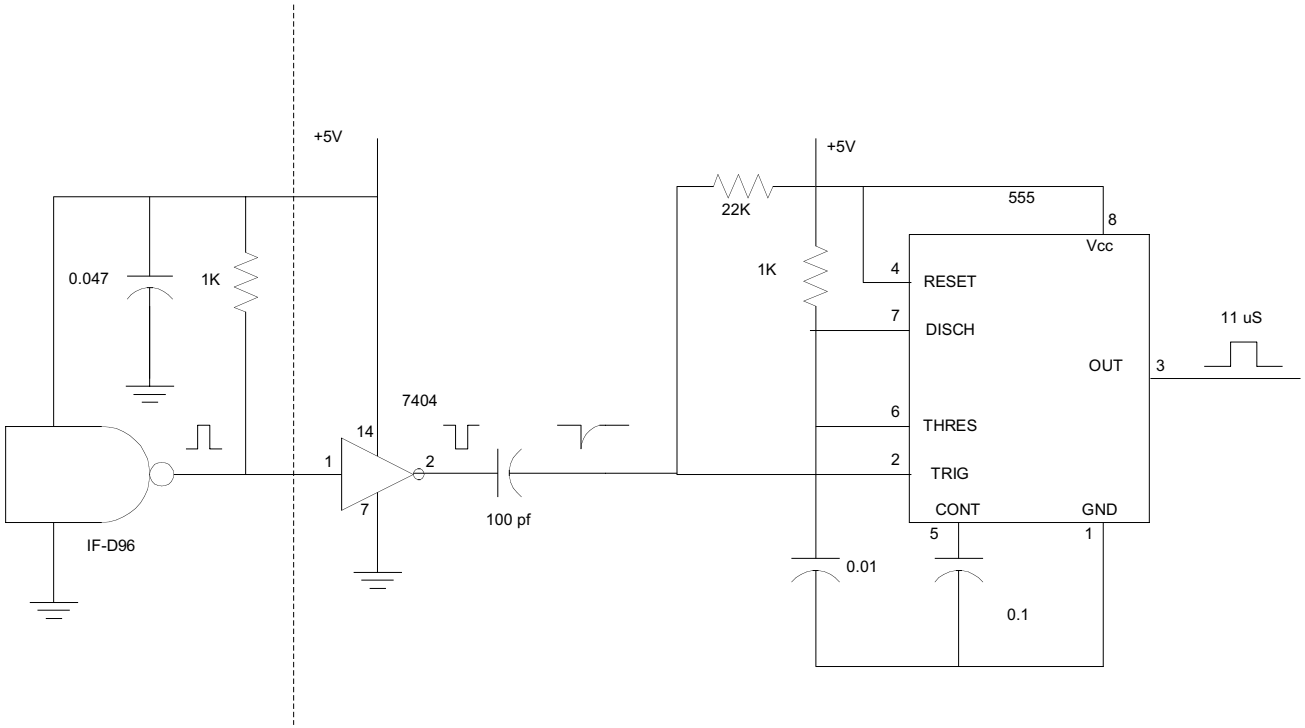

POWERON
1185 Park Center Dr. Ste S
Vista, CA 92083
760-599-0440
760-599-0404 (fax)

POWERON

PHOTODETECTOR BOARD

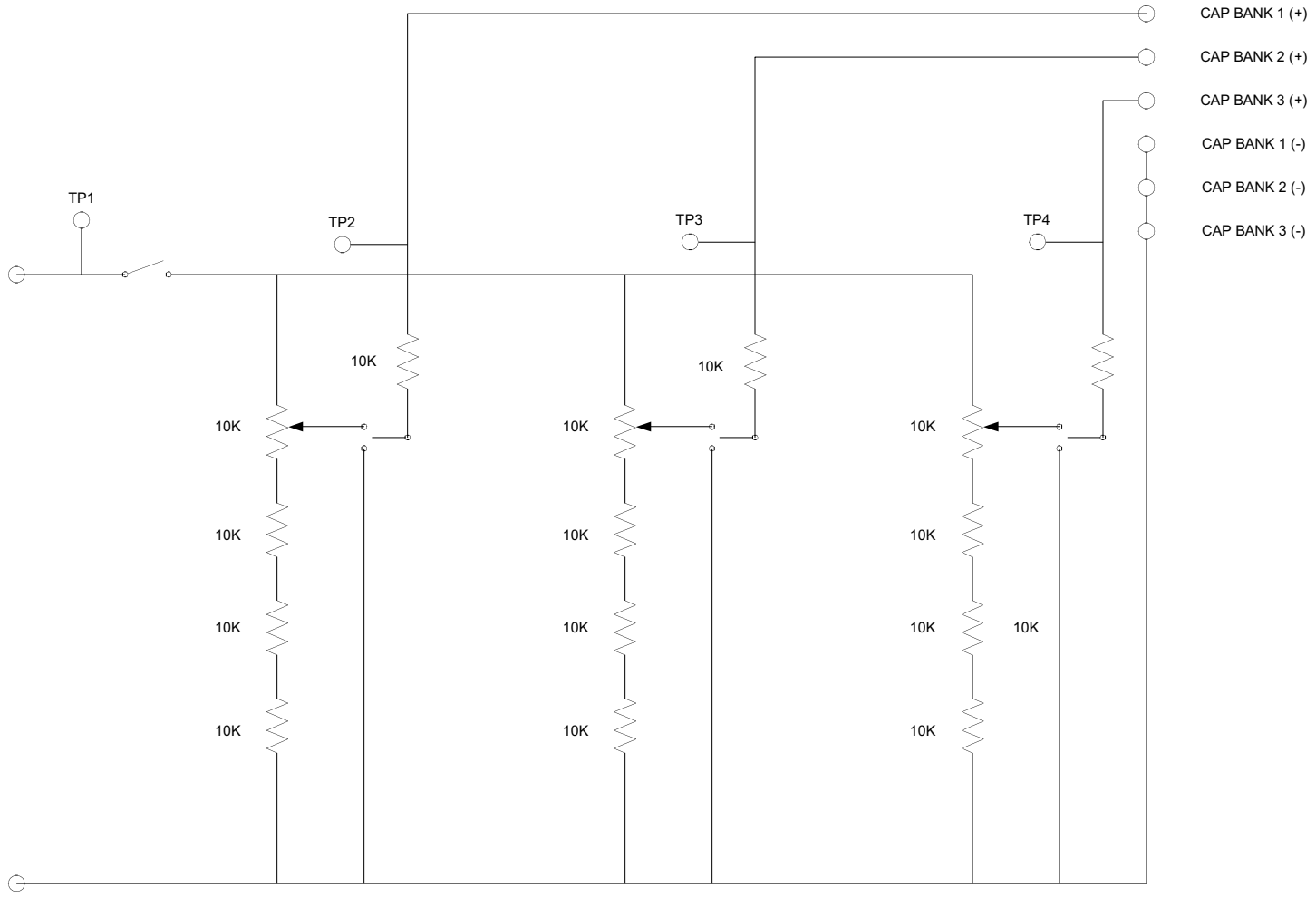

POWERON
1185 Park Center Dr. Ste S
Vista, CA 92083
760-599-0440
760-599-0404 (fax)

POWERON

HIGH VOLTAGE CONTROL

APPENDIX B
STUDIES OF SOLID DT LAYERS IN FOAM

LA-UR-03-0641

Studies of Solid DT Layers in Foam

John D. Sheliak - General Atomics

James K. Hoffer & Drew A. Geller -LANL

presented at the

Second US/Japan Workshop on Target Fabrication, Injection and Tracking

sponsored by

The Department of Energy
Offices of Fusion Energy Sciences & Defense Programs

And hosted by

General Atomics, San Diego, CA

San Diego, CA - February 3-4, 2003

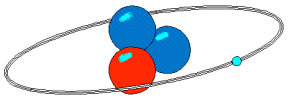

ESA-TSE
Engineering Sciences and Applications Division
Tritium Science & Engineering

Los Alamos
NATIONAL LABORATORY

We have measured the effects of a foam-layered platinum torus on the beta-layered, Solid DT surface roughness

- Both the total RMS surface roughness as well as the l-mode spectral components were measured for several solid DT-in-foam layers that were equilibrated at 19.25 K
- The effects of cell cooling and warming on the solid DT-in-foam surface roughness were measured; cooling from 19.35 K down to 15 K and warming from 15 K to 19.55 K
- Our studies show an average smoothing of 50% for total RMS, and 60% for ∑ (modes 10-100), compared to results from recent DT aging experiments done in our 2-mm beryllium torus. We also observed an average smoothing of 80% for ∑ (modes 50-100) with DT-in-foam layers.

There are several hypotheses concerning the effects of an intermediate foam layer on the inner solid DT layer

- Beneficial effects:
  - **A smoother interior surface**
    - Because of the fine cell structure of the foam, freezing should begin with the formation of many small, randomly-oriented crystallites. These crystallites should propagate into the pure DT solid layer, hence there should be no tendency to form large crystalline facets at the solid-vapor boundary.
  - **Supercooling of the liquid should not occur**
    - With millions of nucleation sites presented by the foam, the liquid does not supercool as is observed in smooth plastic spheres without a foam layer.
- Detrimental effects:
  - **If irregular, the overall shape of the foam may affect the shape of the solid DT.**
    - But I'm guessing that the gross shape of the foam will not influence the shape of the solid DT layer, because the foam is a thermal insulator and will not disturb the isotherms defined by the isothermal boundary (i.e., the metallic cell boundary in my cylindrical experiments or the 'layering sphere' utilized for spherical targets at Omega.)
  - **The polymeric foam material may be damaged by beta activity and decompose.**
  - **DT voids in the foam cells may become trapped**
    - The solid DT is 12.5% denser than liquid. A void space (full of DT vapor) therefore develops whenever a cell full of liquid is frozen. (When symmetrized by beta-layering, the void in a single spherical shell will extend exactly half-way across the cell.) Voids first formed in the foam cells tend to propagate inwards to the central vapor space. If the inner edge of a foam cell is blocked by a cell wall (i.e., if the foam is not completely 'open-celled'), then the void may get 'stuck'. Stuck voids may not be too detrimental, because they are sub-micron in size. But a secondary effect might be a very slow approach to equilibrium wrt the DT layer thickness.

The foam-lined torus permits clear optical observations of the DT layer:

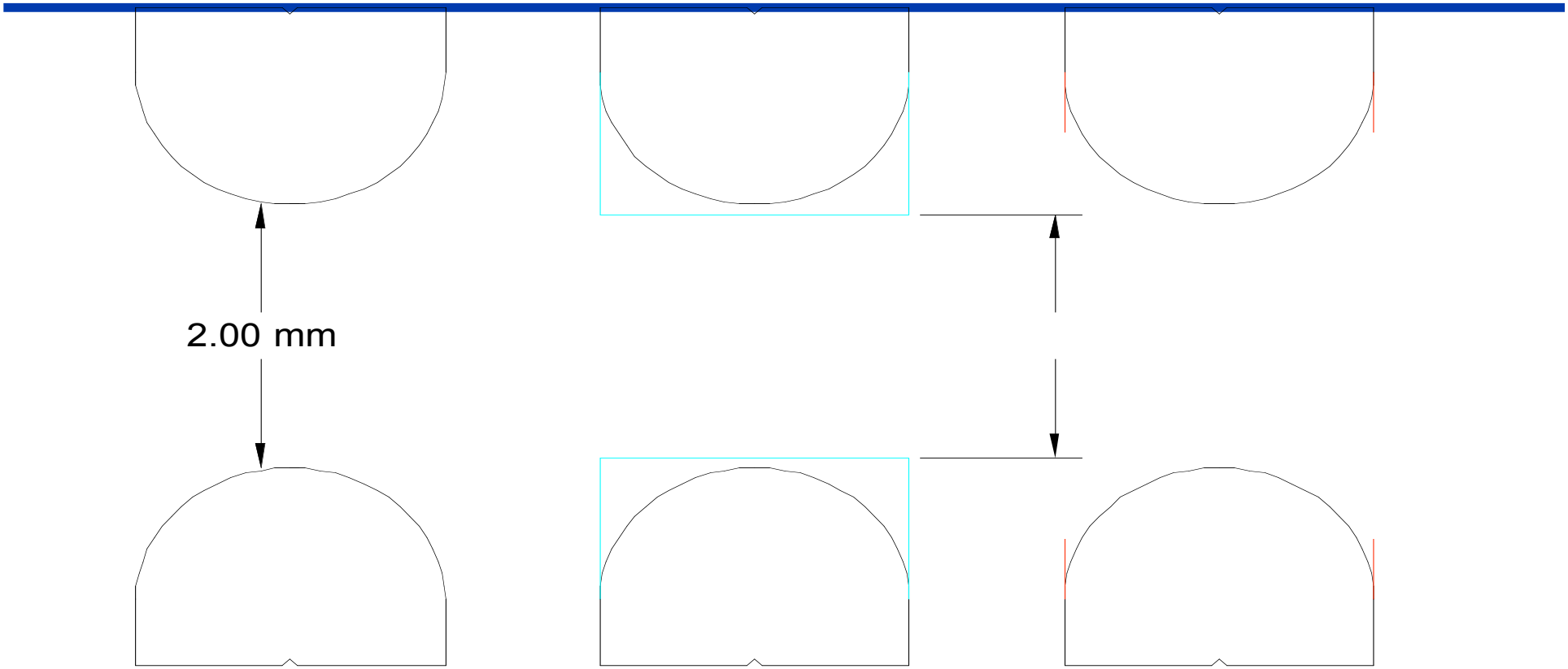

Empty torus
side view
(windows not shown)

Filled with foam to yield a 75 micron-thick layer at the waist, then filled with liquid DT

Filled with DT and beta-layered to yield a solid layer 100 microns thick.

GENERAL ATOMICS

Los Alamos
NATIONAL LABORATORY

Several 2 mm tori were fabricated from pure Pt

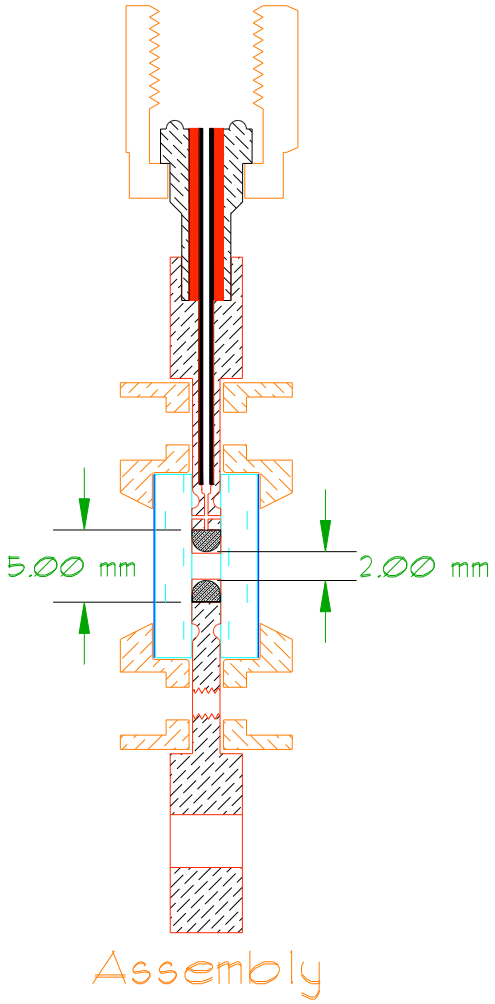

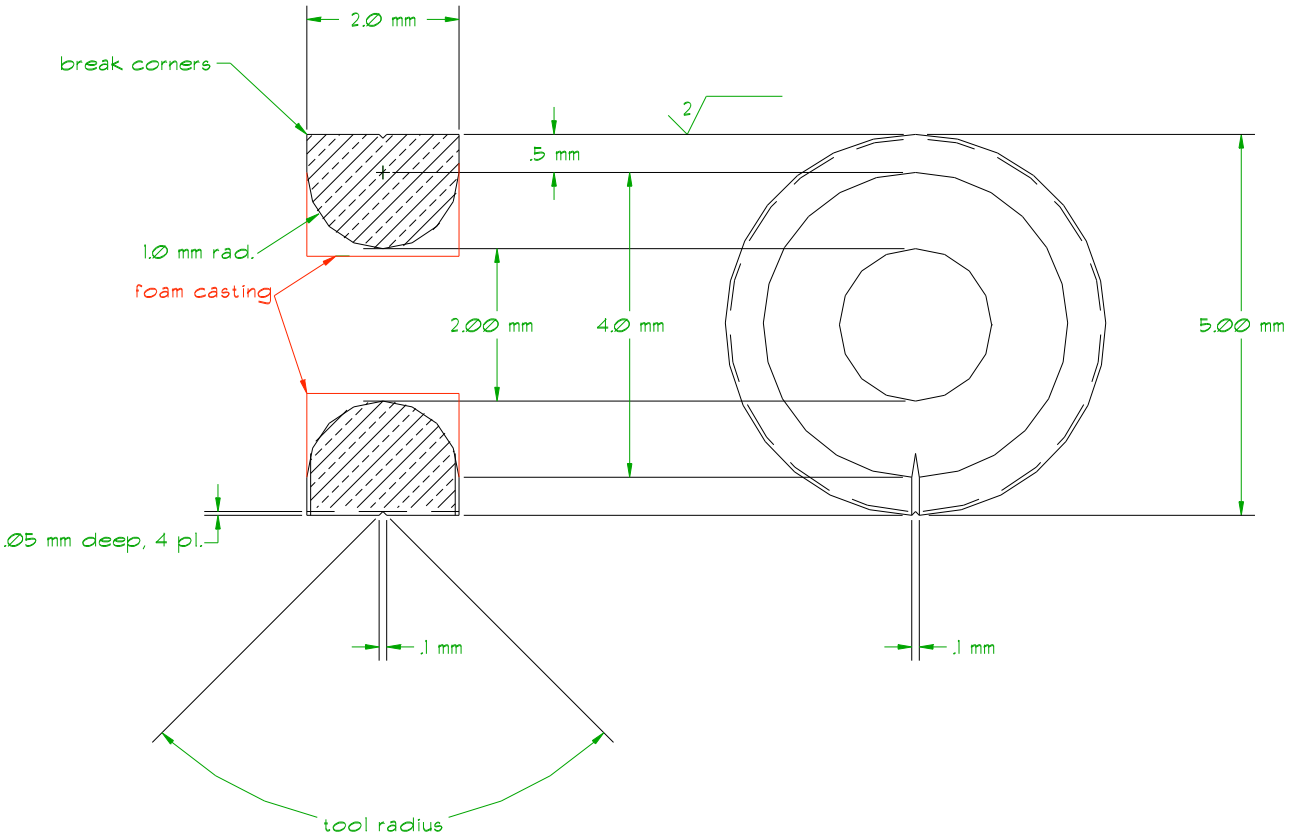

GENERAL ATOMICS

Los Alamos NATIONAL LABORATORY

At Sandia, Diana Schroen & co-workers added ~70-□-thick RF foam layers to four tori:

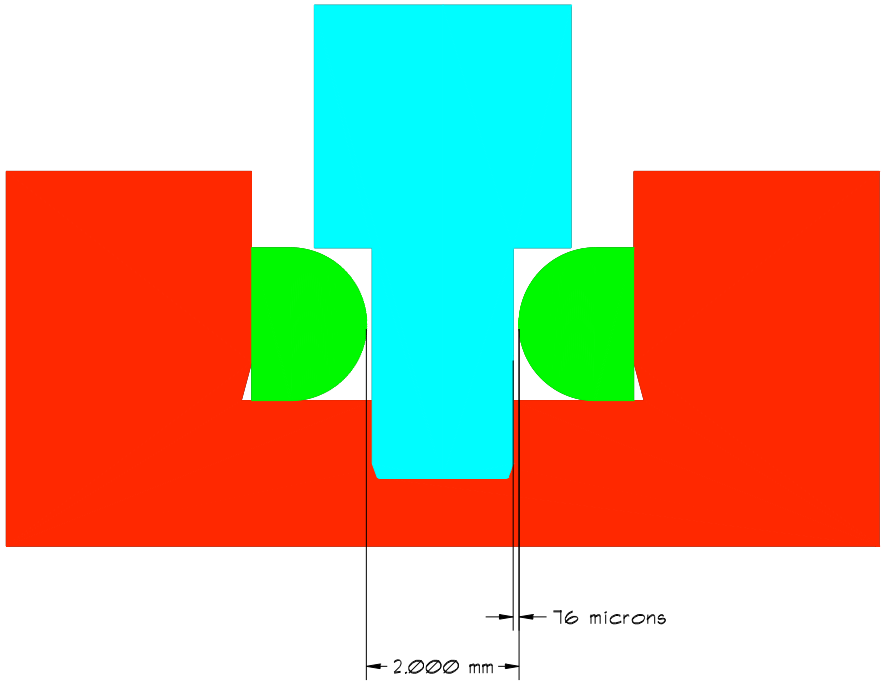

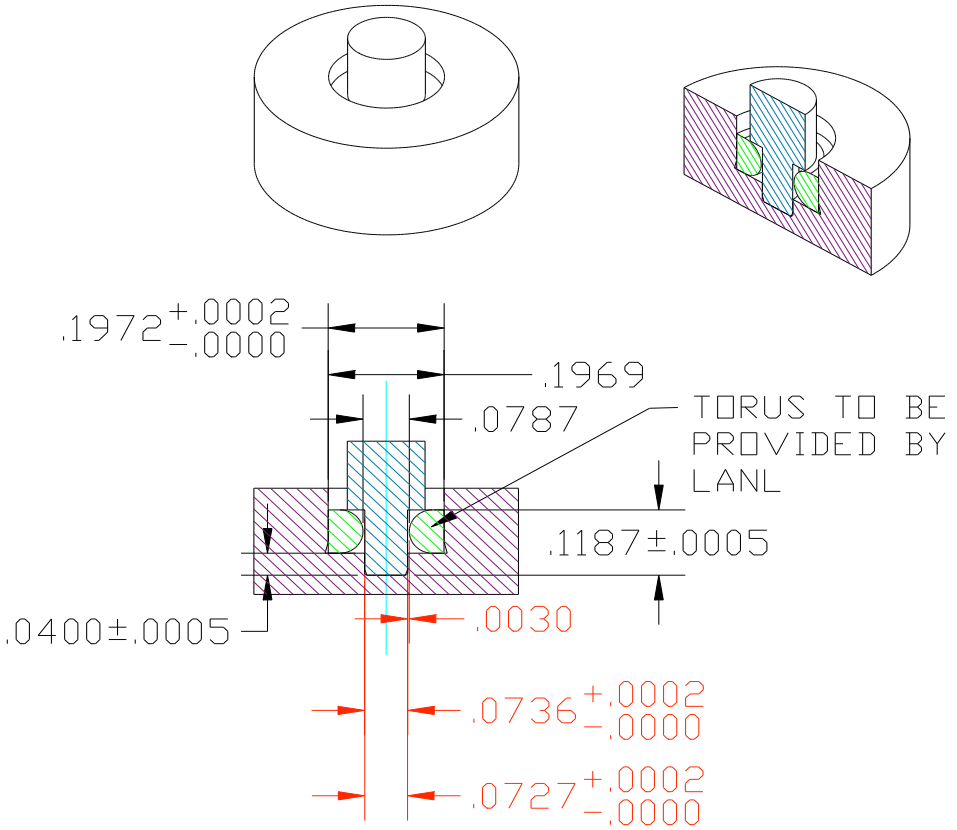

GENERAL ATOMICS

Los Alamos NATIONAL LABORATORY

We measured the foam thickness by 'subtracting' an image of the unfilled Pt torus. We then chose cell 'C' based on:

- overall symmetry,
- average foam layer thickness, and
- relative lack of defects at the toroidal waist

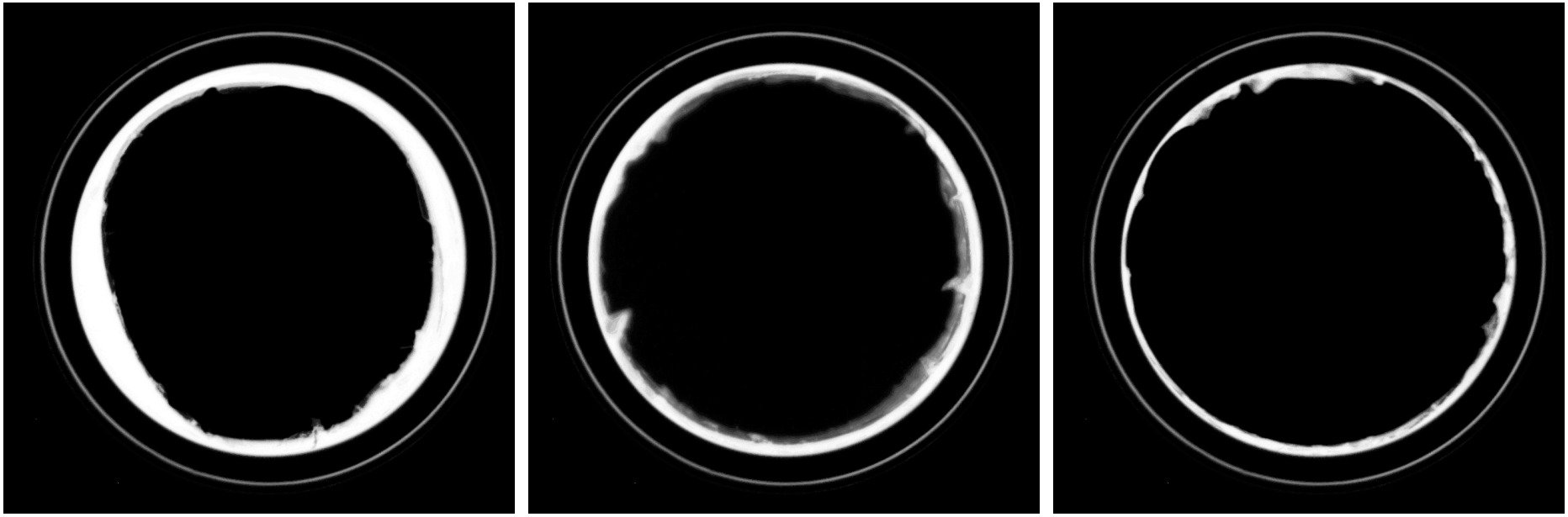

Cell 'B' - average d = 125μm

Cell 'C' - average d = 74 μm

Cell 'D' - average d = 47 μm

GENERAL ATOMICS

Los Alamos NATIONAL LABORATORY

Foam Thickness Decreased from 74 µm over the course of several experiments, then stabilized at about 43 µm

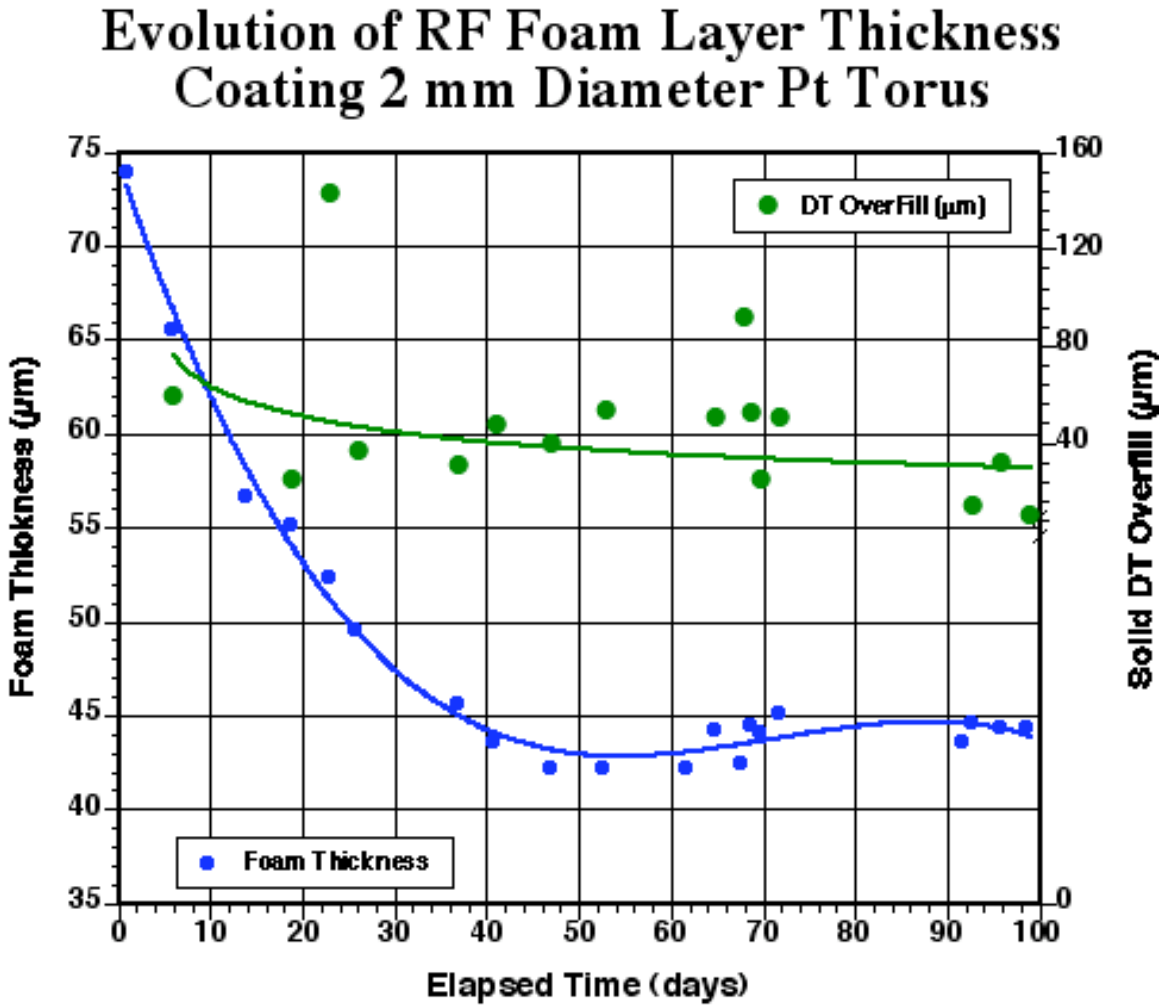

GENERAL ATOMICS

Los Alamos NATIONAL LABORATORY

Once the solid layer has equilibrated, we can show the pure DT layer by subtracting the empty foam image.

Note that the solid DT ignores the defects in the foam!!!

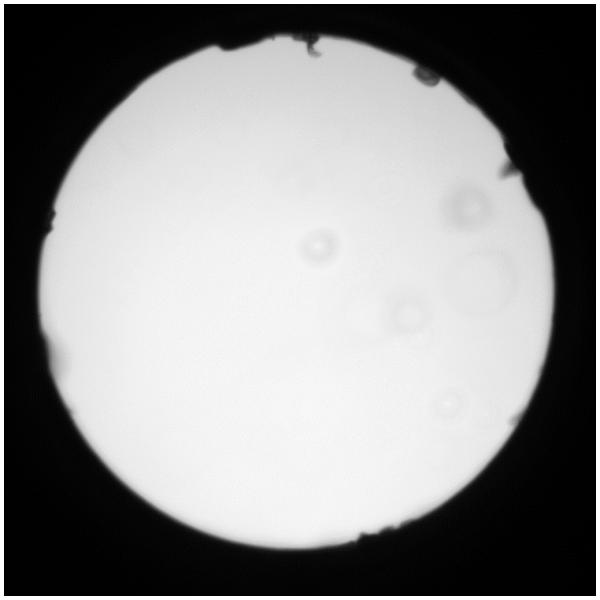

empty foam

98 μm DT layer (total)
~50 μm is 'pure', while the rest resides in the foam

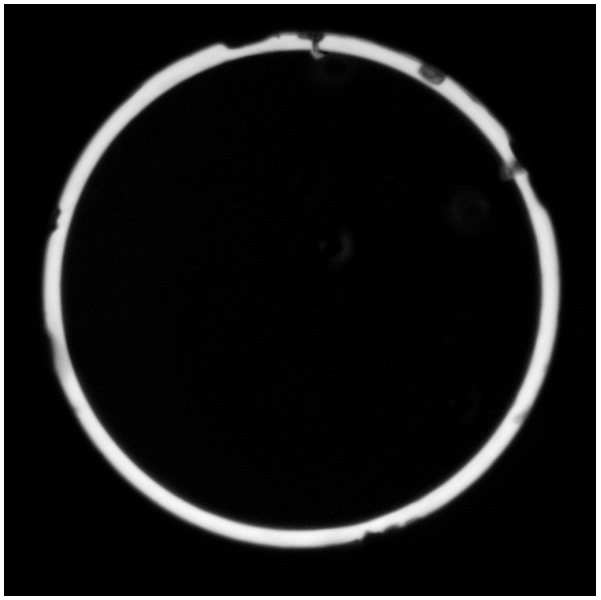

Empty foam – DT Layer

GENERAL ATOMICS

Los Alamos NATIONAL LABORATORY

This is a typical solid DT layer equilibration at 19.25 K in the foam-layered Pt torus

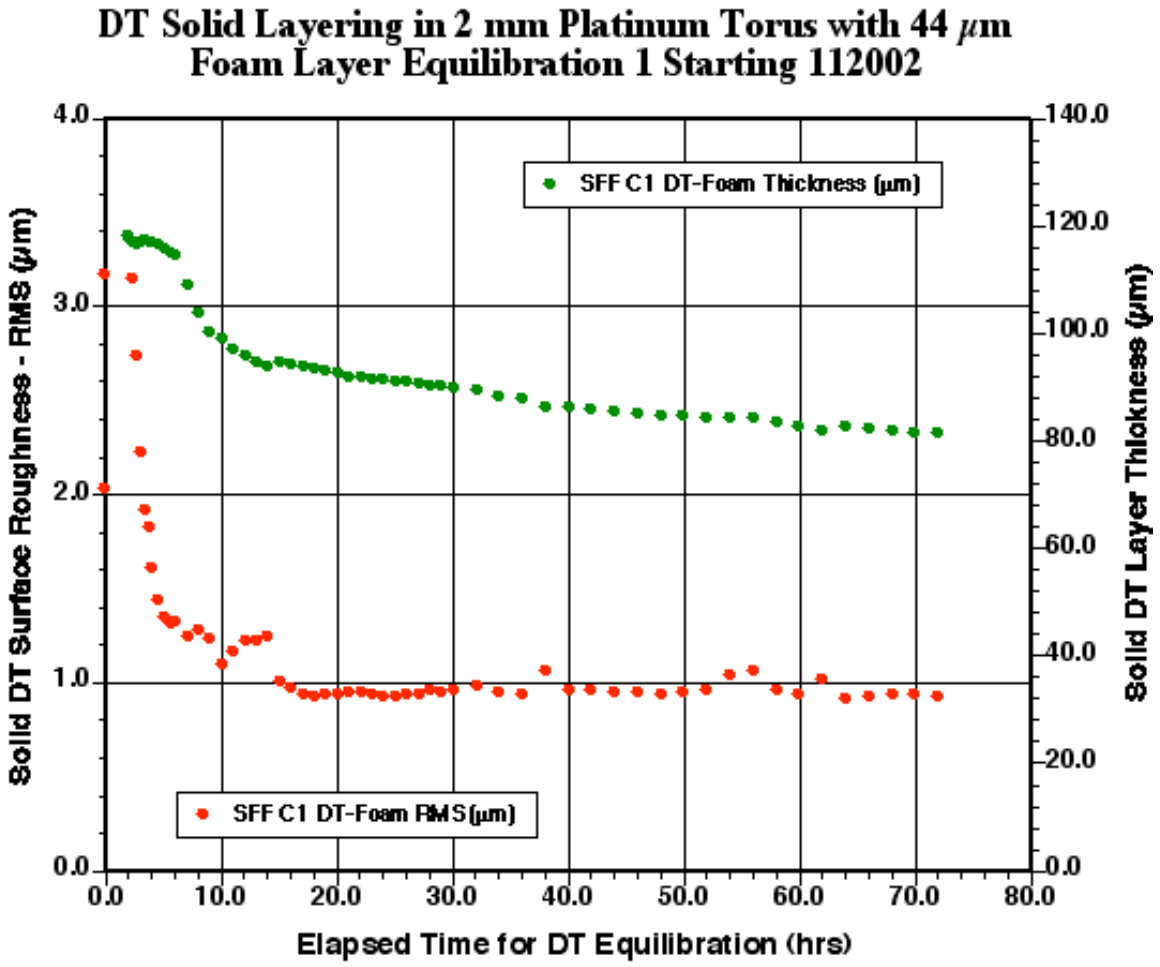

GENERAL ATOMICS

Los Alamos NATIONAL LABORATORY

But the solid DT surface is much smoother than we have thus far observed in this geometry

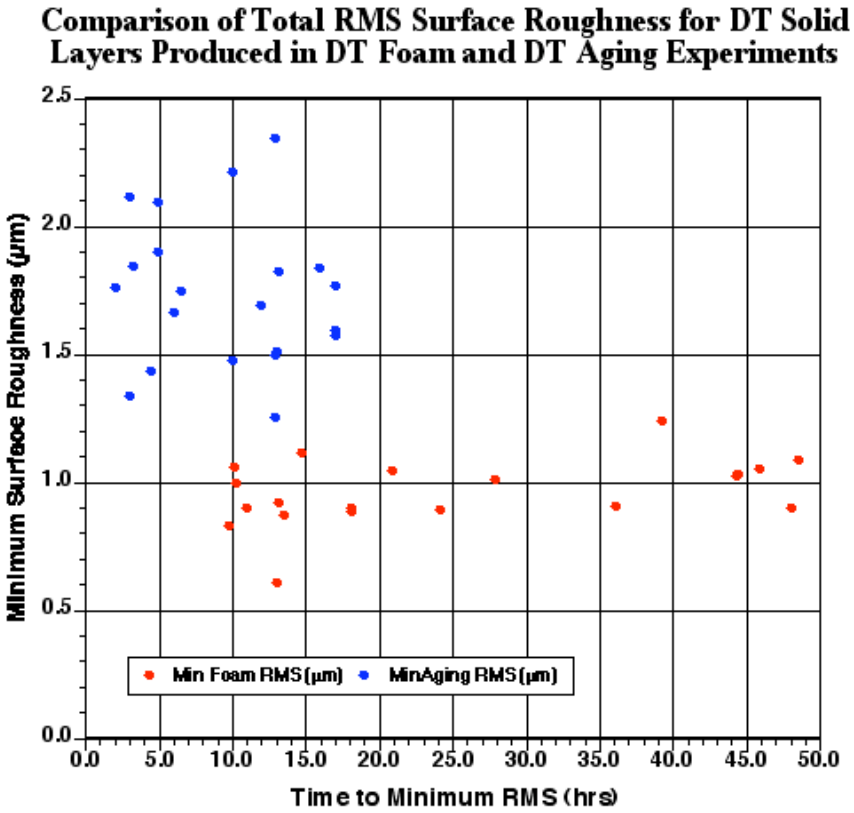

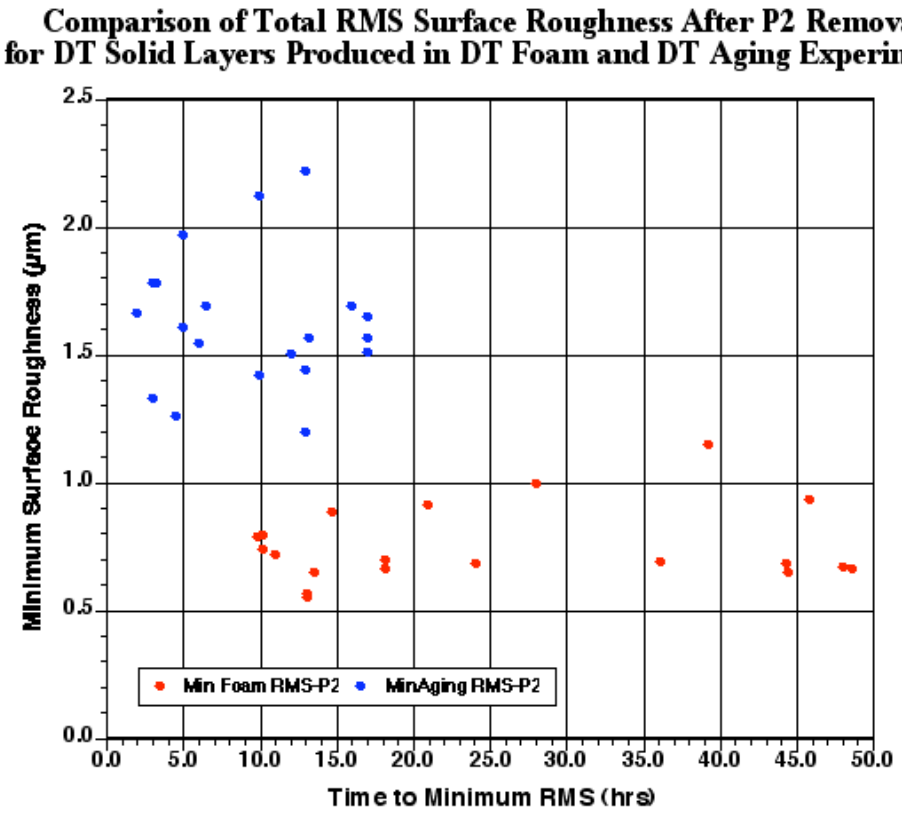

GENERAL ATOMICS

Los Alamos NATIONAL LABORATORY

The mode 2 amplitude is responsible for about 20% of the total rms roughness. Some of this is due to the fact that we now cannot line up the empty torus 'on axis'.

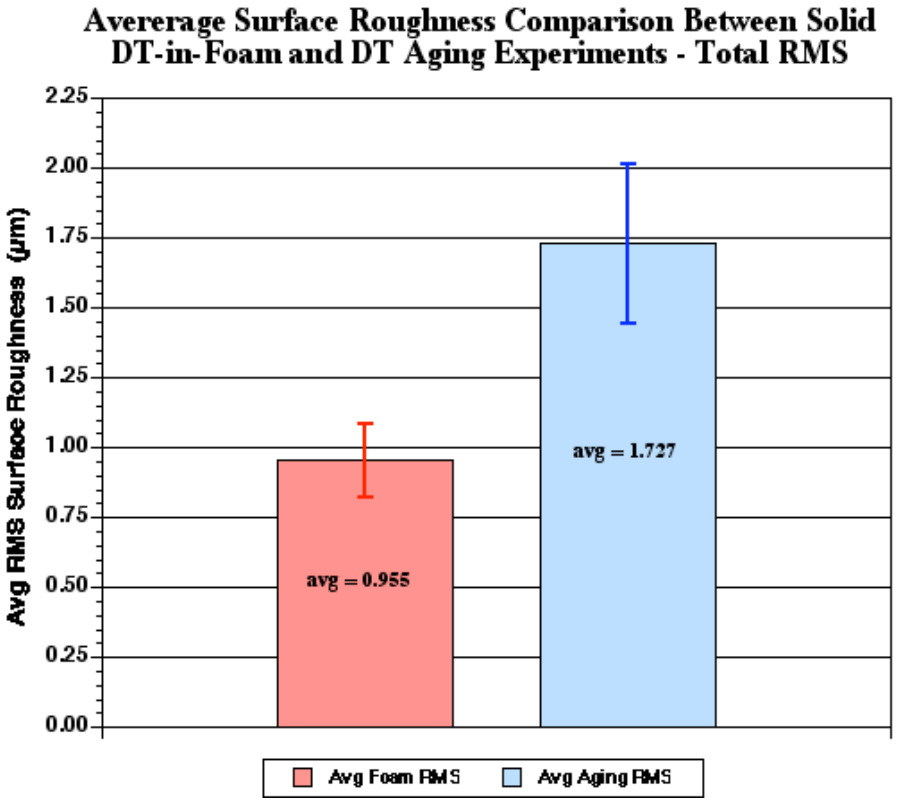

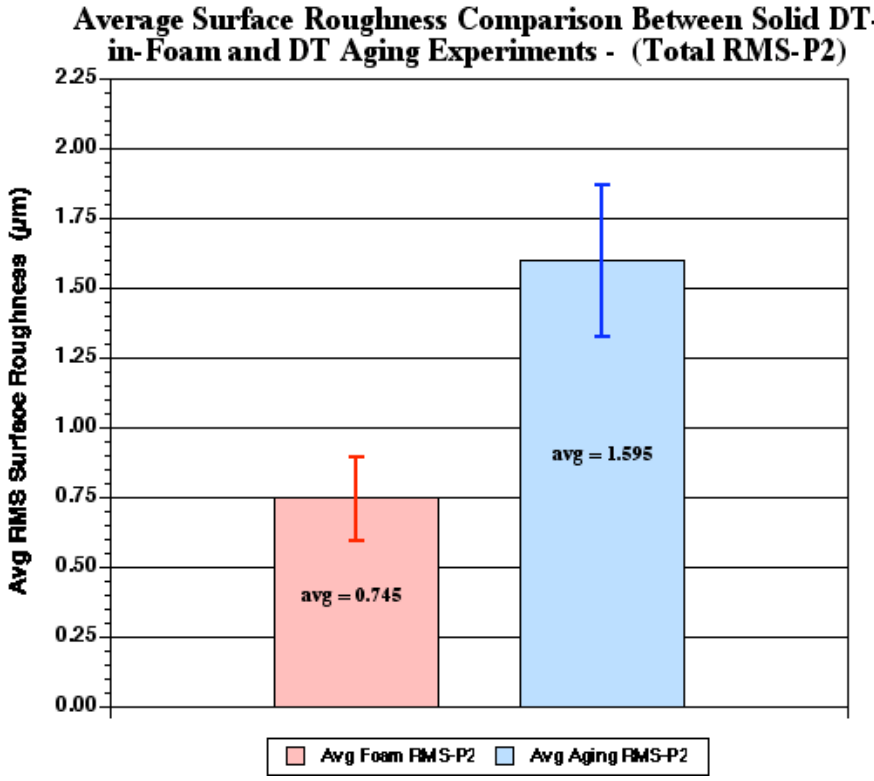

GENERAL ATOMICS

Los Alamos NATIONAL LABORATORY

By plotting a ‘reverse sum’ of modes, the modal spectrum can be seen. The presence of the foam is dramatically reducing the roughness power at l-modes 10-100.

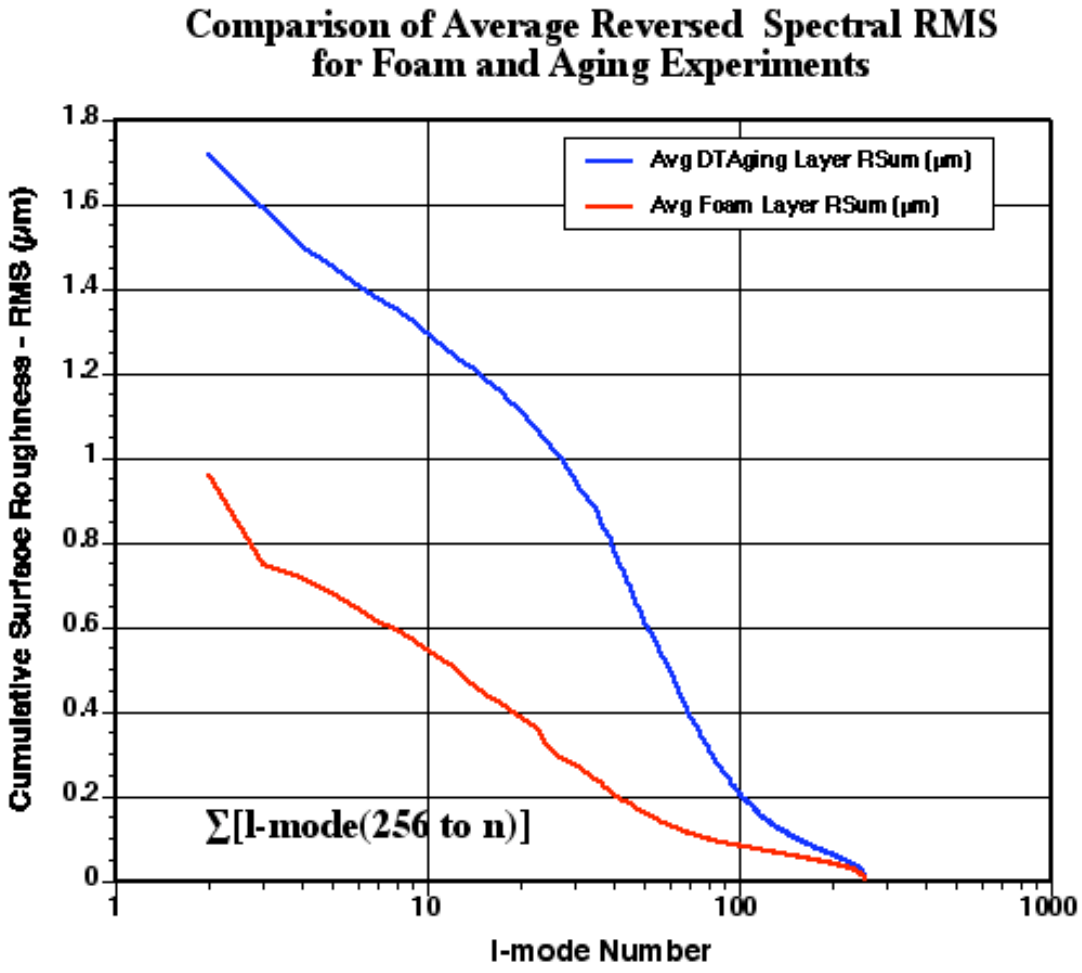

GENERAL ATOMICS

Los Alamos NATIONAL LABORATORY

This compares the 'best' of our previous results with several of our results in foam. Simply put, we have never seen such a smooth beta-layer!!

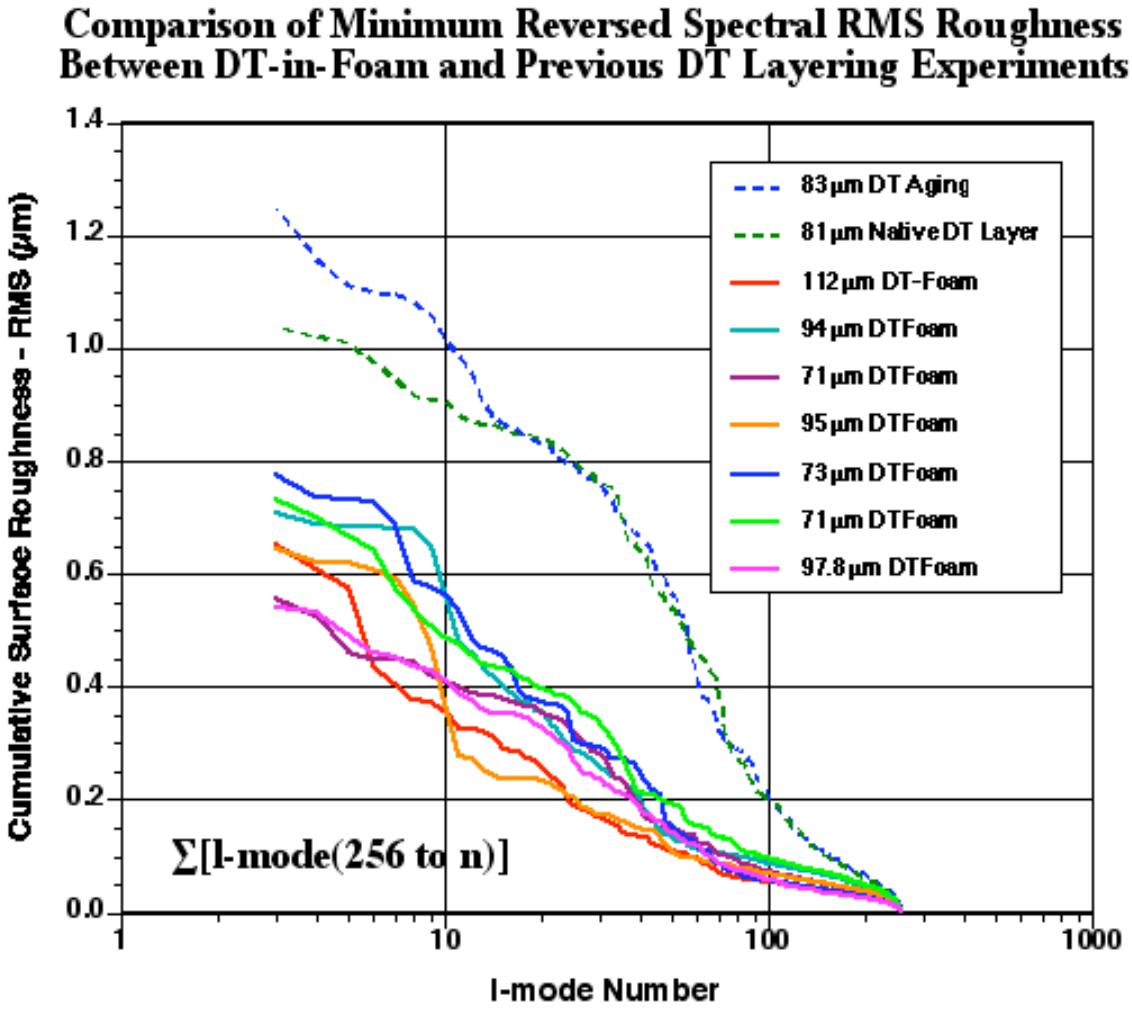

GENERAL ATOMICS

Los Alamos NATIONAL LABORATORY

This compares the best two foam layers with the best of two previous experiments, and the LLNL data in spheres, where the solid DT layer is grown as a 'single crystal.'

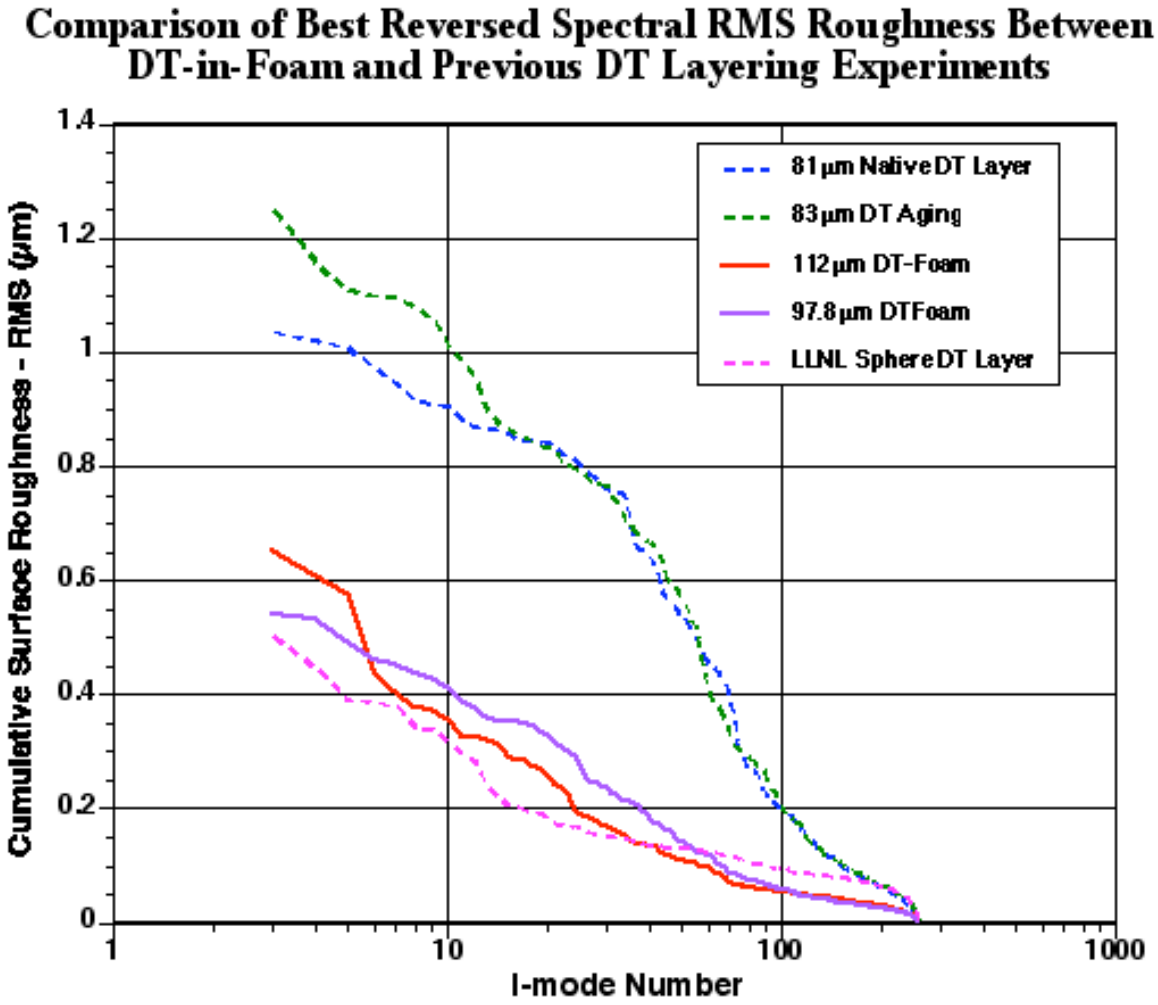

GENERAL ATOMICS

Los Alamos NATIONAL LABORATORY

As a function of time, the 'disappearance' of mid and higher modes is precisely what we do not observe when no intermediate foam layer is present.

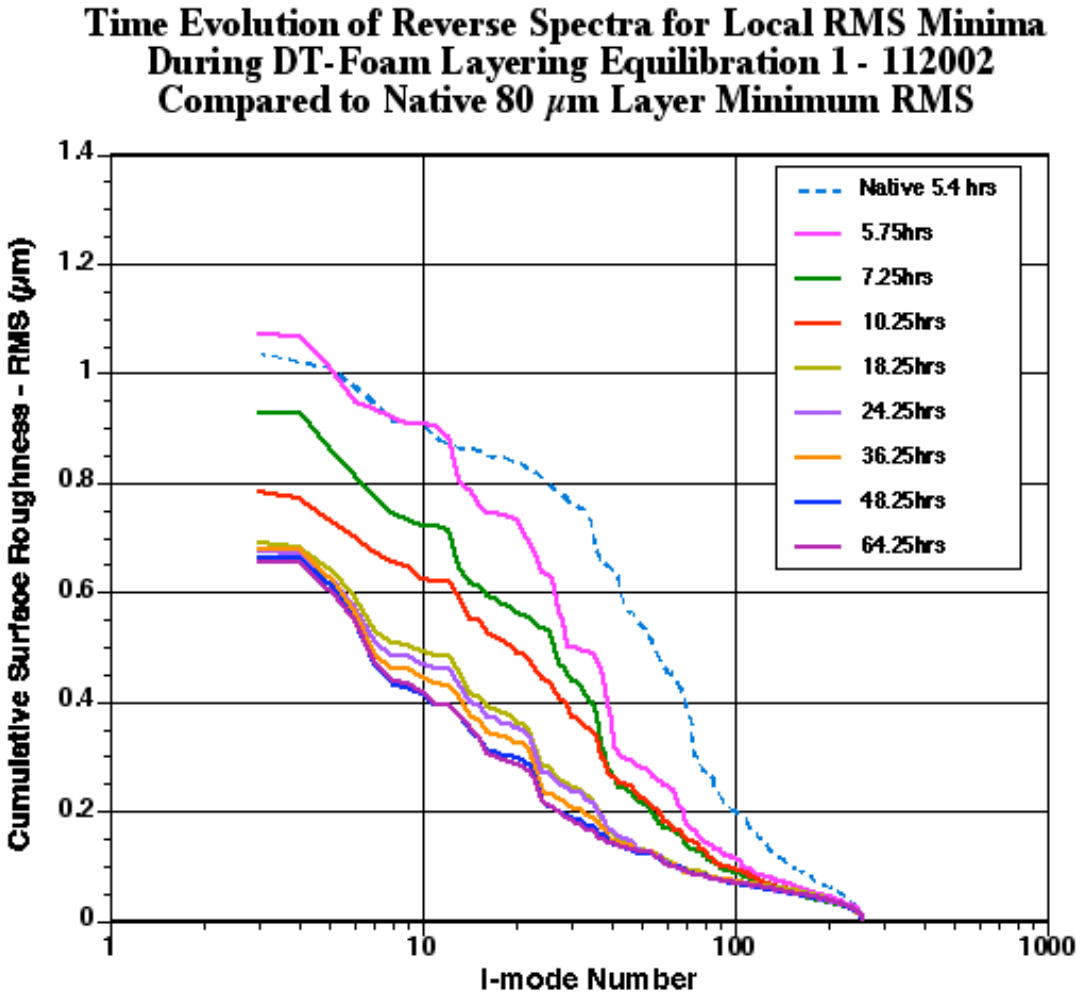

GENERAL ATOMICS

Los Alamos NATIONAL LABORATORY

We also measured the effects of cooling the layer from initial equilibrations at 19.25 and 19.35 K down to 15 K

- Cooling an equilibrated DT solid layer from 19.25 to 16 K increased the average surface roughness 50-75% (using the same initial equilibration temperature); but on average the layers were still as smooth as, or smoother than those from our best previous experiments
- Warming the cooled DT solid layer back to 19.45 K does not reverse the roughening that was observed during the cooling process, although some smoothing is observed (~15%).
- Roughening appears to be dominated by l-modes 10 to 50 and P2; although ∑(l-modes 10-50) continue to roughen during re-warming, whereas P2 virtually disappears during re-warming

This is a typical solid DT layer equilibration at 19.25 K with decreasing stepped temperature ramping to 16 K

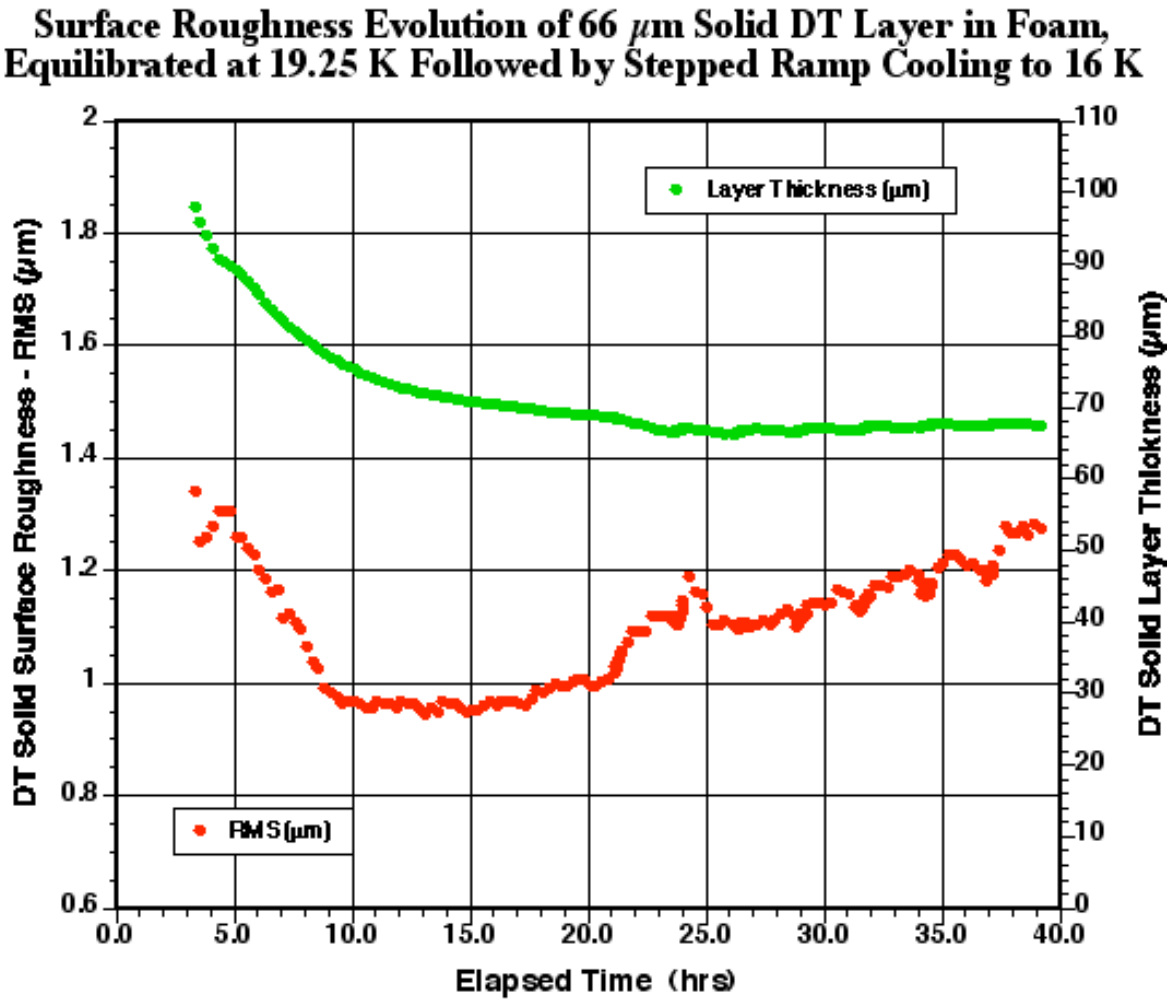

GENERAL ATOMICS

Los Alamos NATIONAL LABORATORY

Stepped-ramp cooling to16 K increased the surface roughness by about 50%, but RMS is still ≤ 1.4 μm

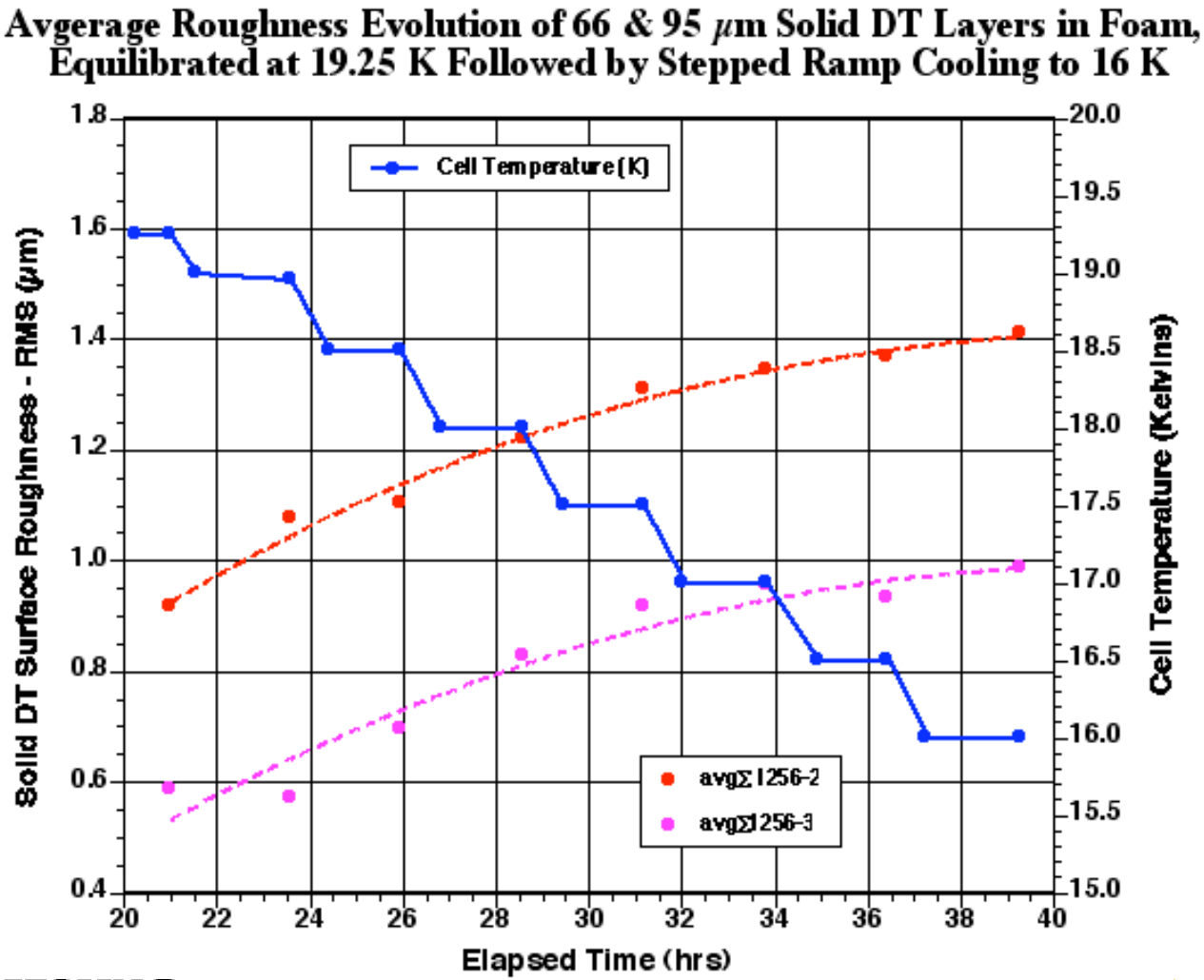

GENERAL ATOMICS

Los Alamos NATIONAL LABORATORY

This is the solid surface total RMS roughness as a function of DT cell temperature

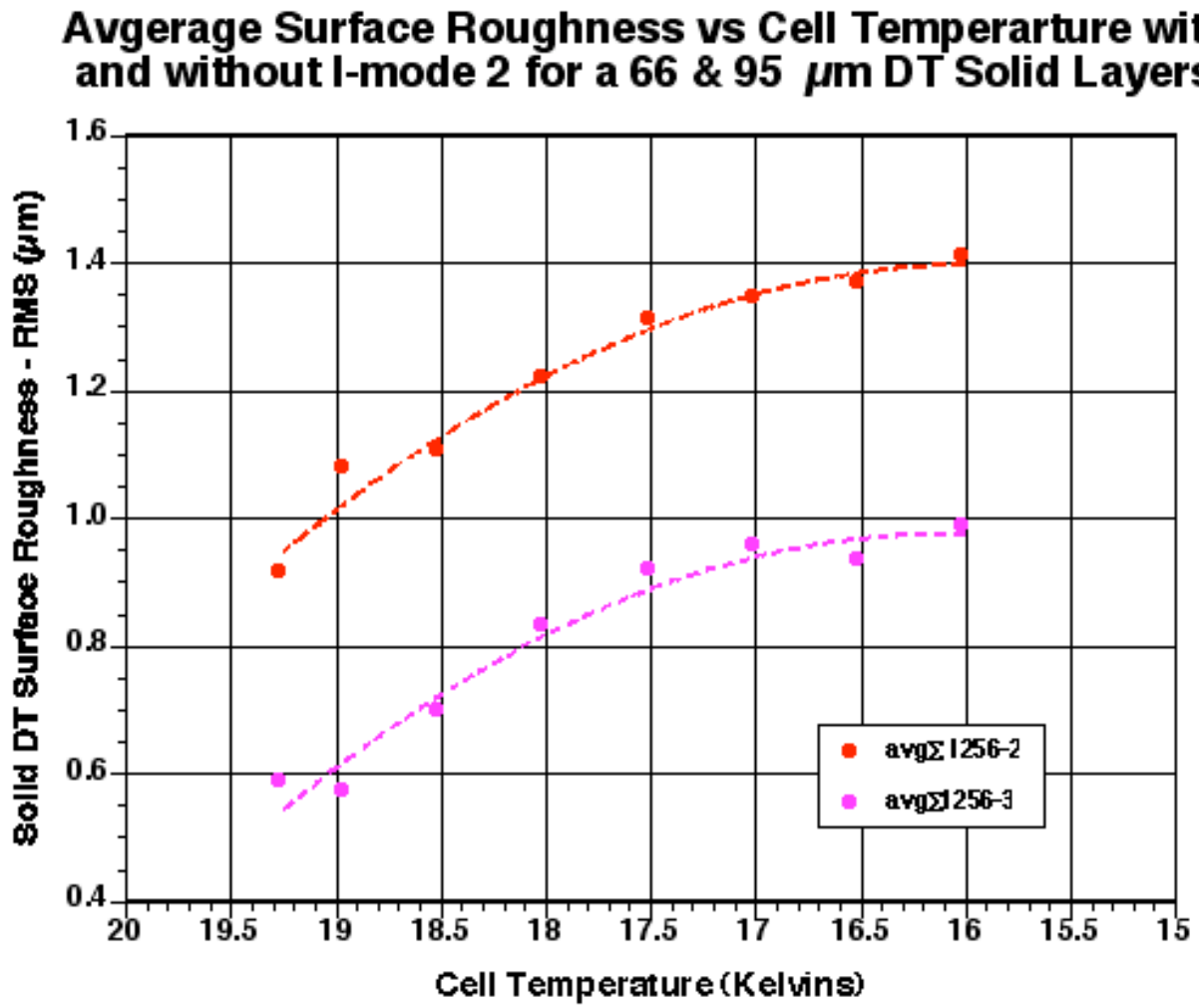

GENERAL ATOMICS

Los Alamos NATIONAL LABORATORY

This ‘reverse sum’ of the l-mode roughness shows the DT-in-foam roughening process, excluding P2 contribution

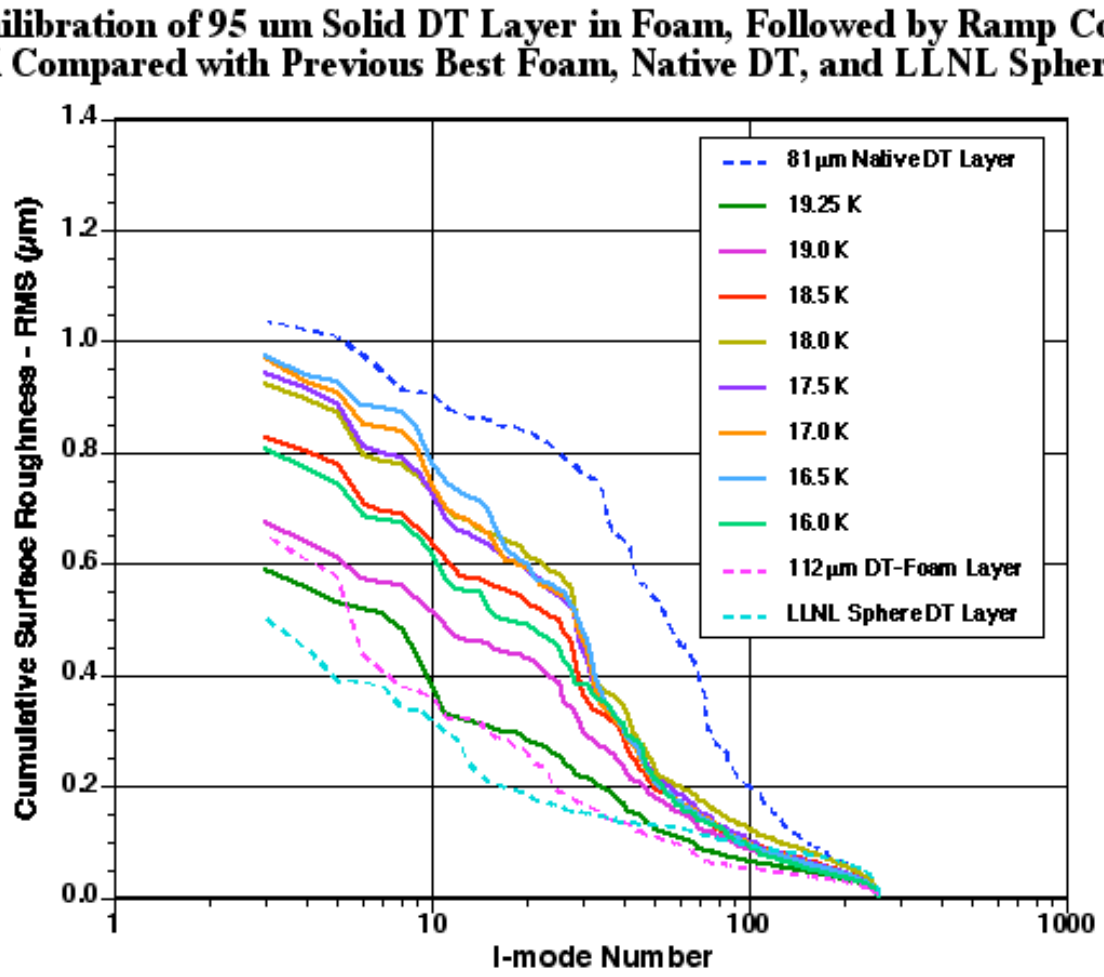

GENERAL ATOMICS

Los Alamos NATIONAL LABORATORY

Solid DT roughening that is observed during the cooling process, smoothens some but does not 'heal' completely

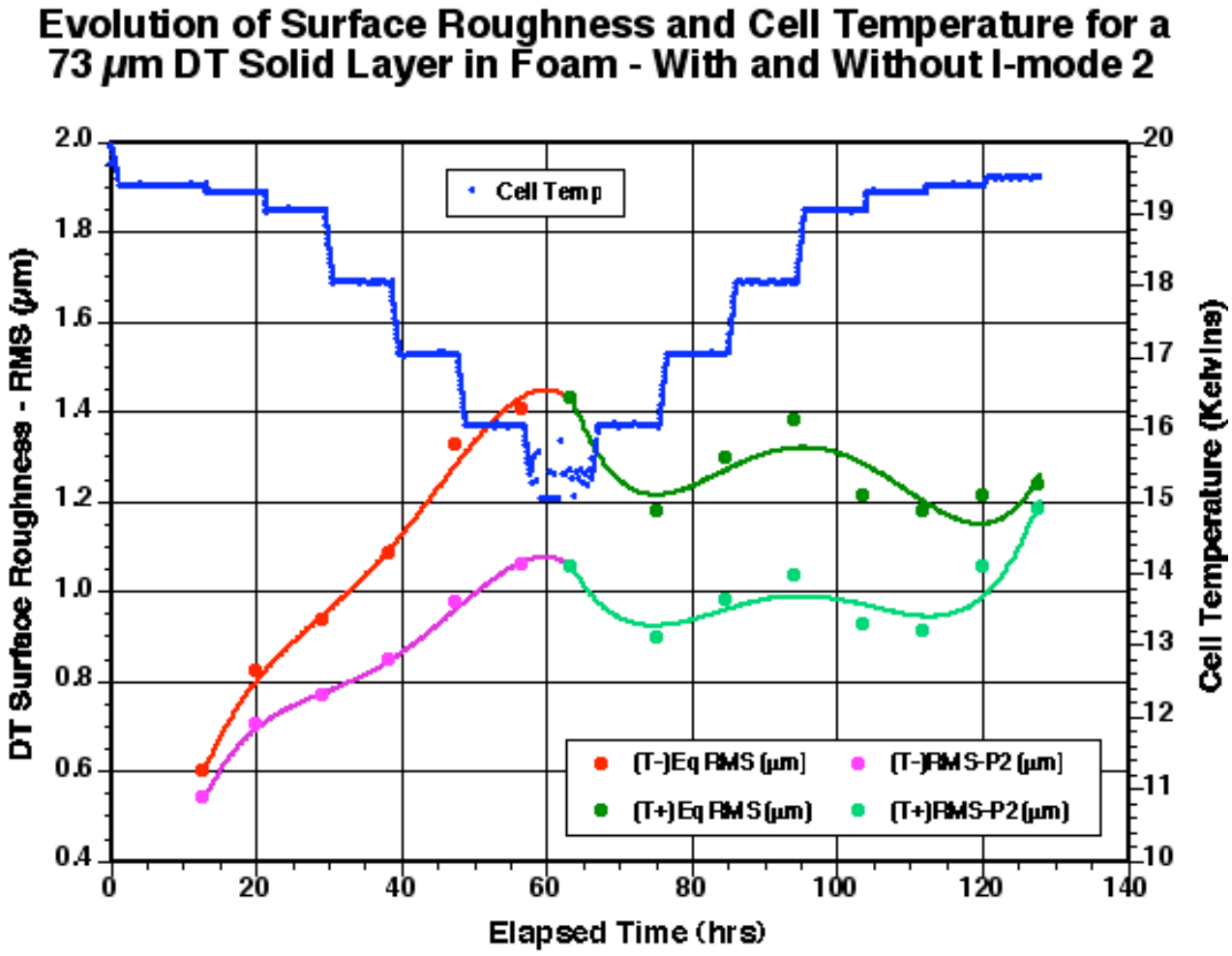

GENERAL ATOMICS

Los Alamos NATIONAL LABORATORY

Roughening appears to be dominated by modes 10 to 50 & mode 2 (although P2 nearly vanishes during re-warming)

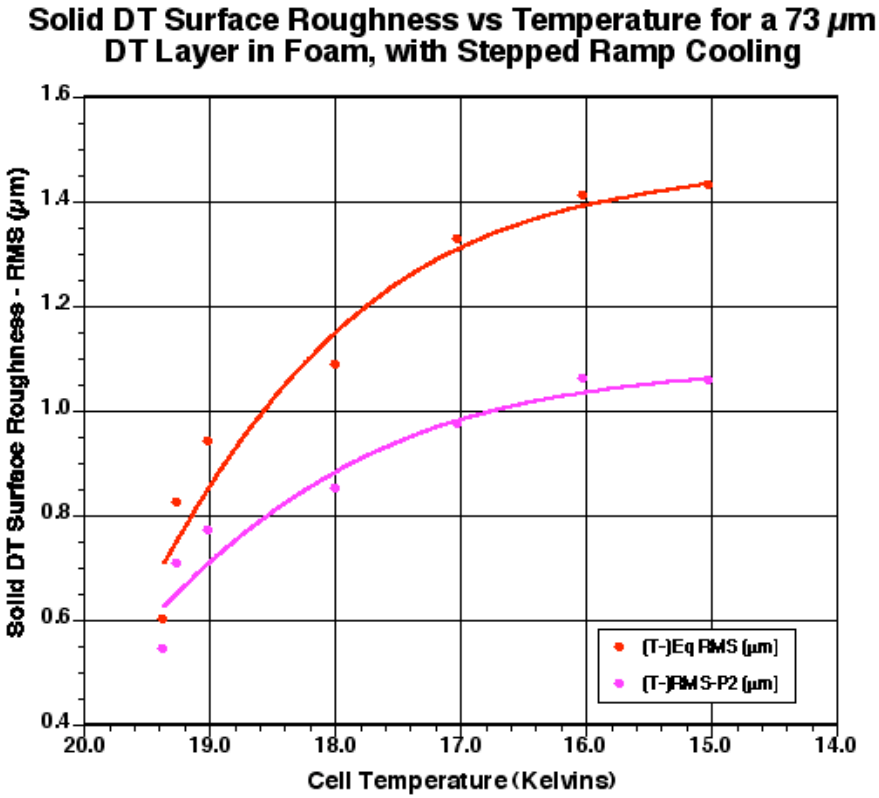

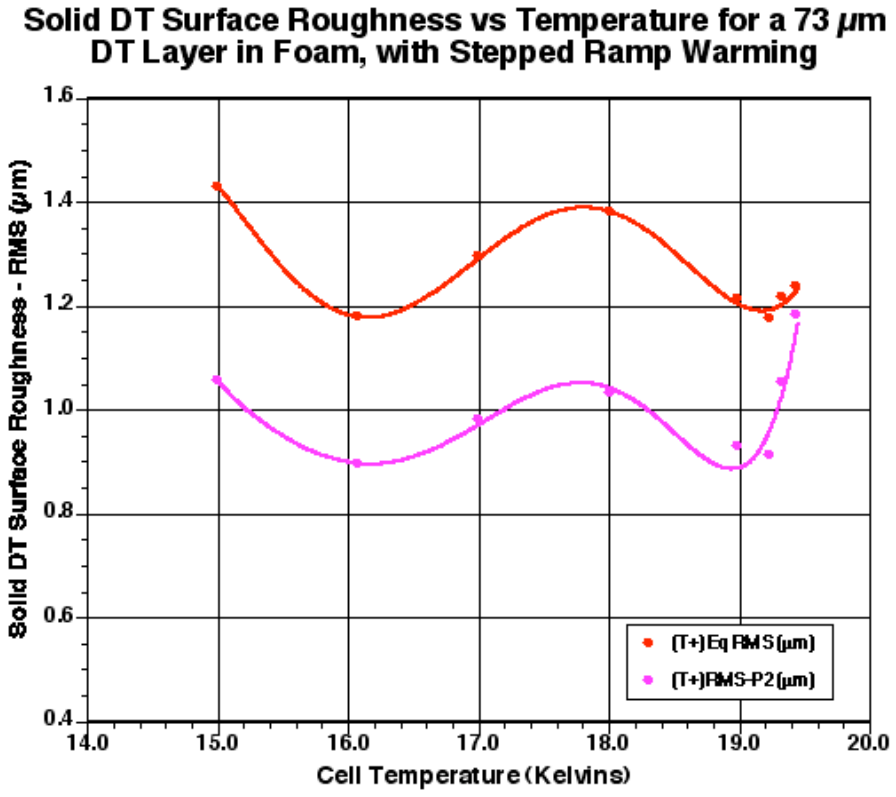

GENERAL ATOMICS

Los Alamos NATIONAL LABORATORY

Solid Surfaces do roughen during cooling, and smoothen slightly when warming; yet the surface is as good as (or better) than those from our best previous experiments!

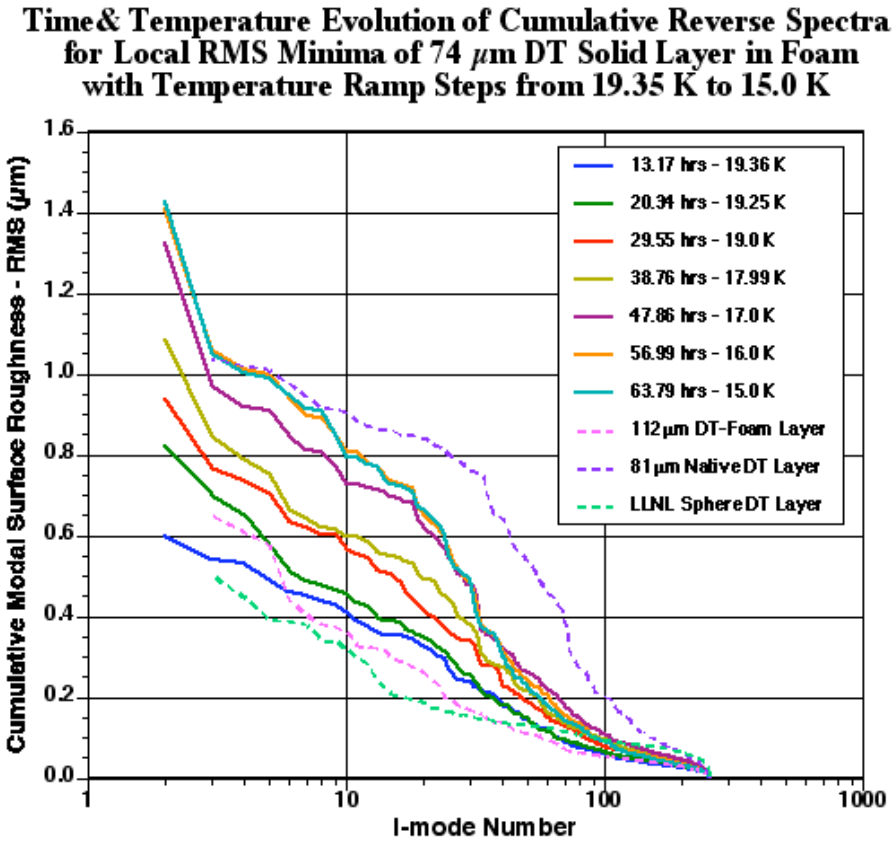

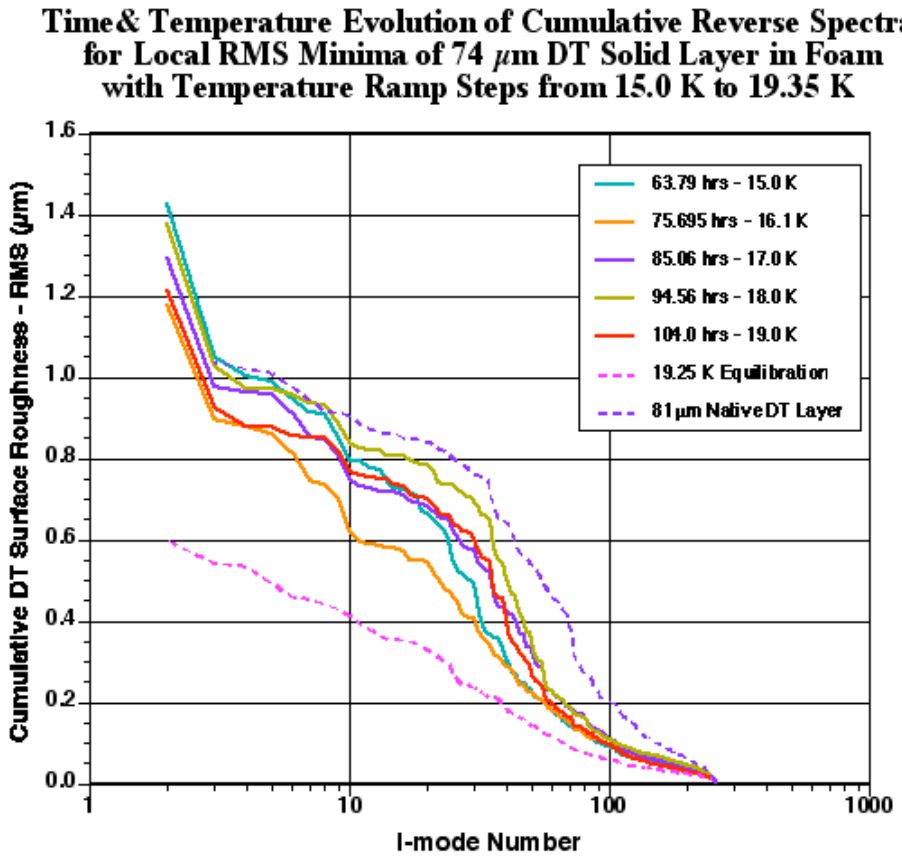

GENERAL ATOMICS

Los Alamos NATIONAL LABORATORY

This shows the roughening effects of the cooling and re-warming process in terms of segmented l-modes [$\sum(l_u-l_l)$]

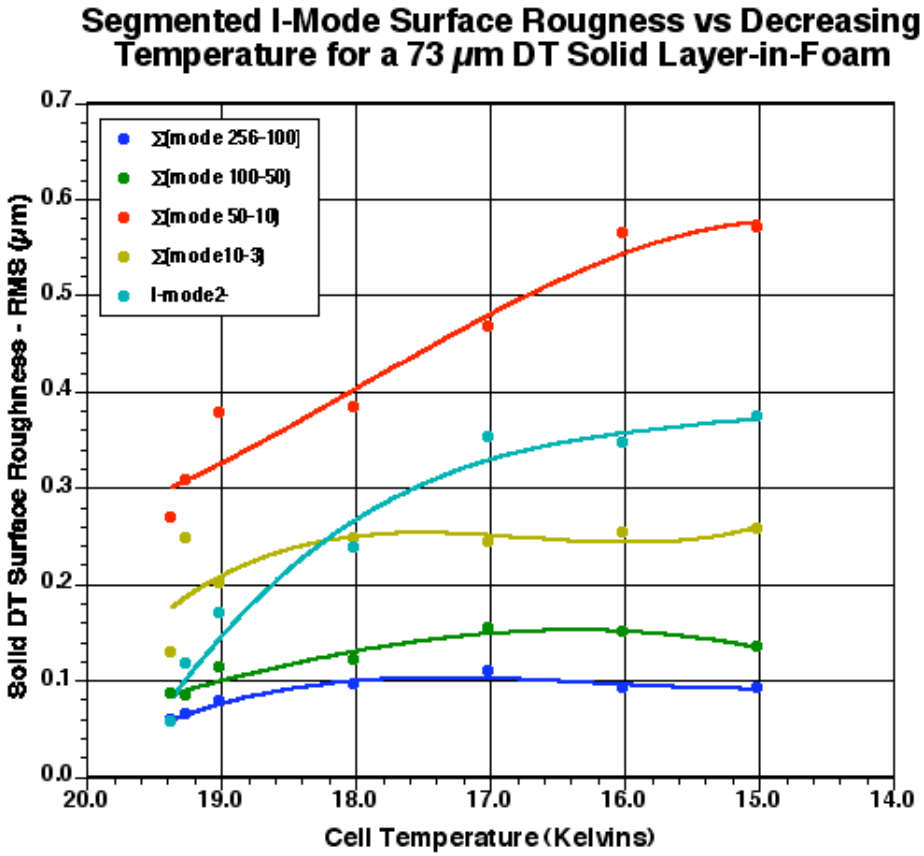

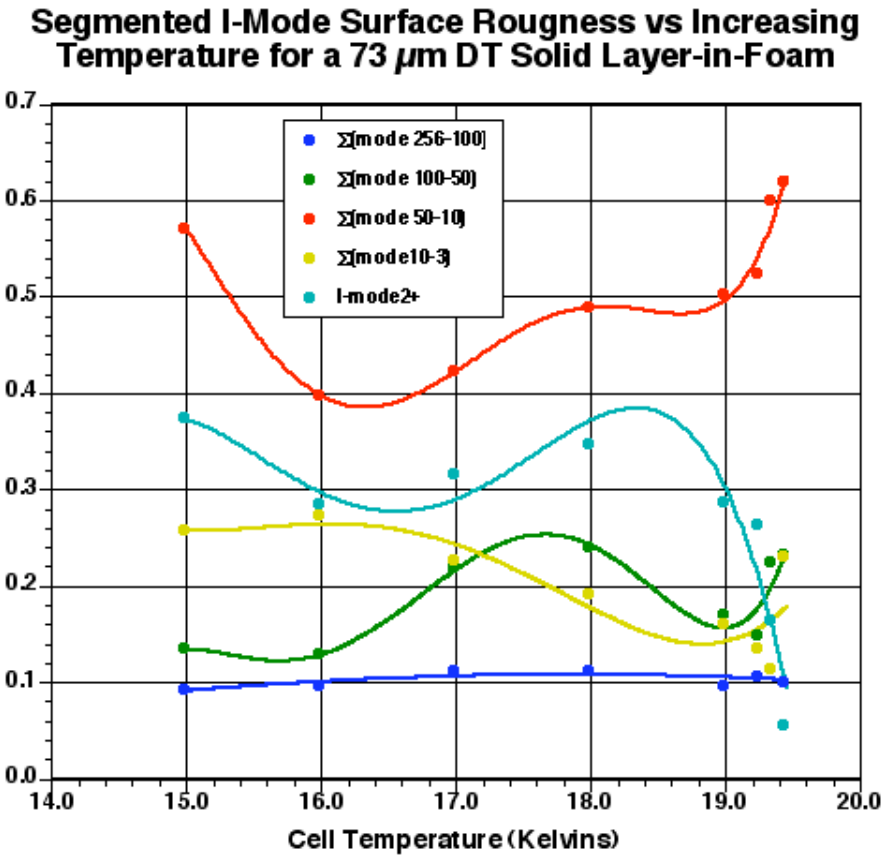

GENERAL ATOMICS

Los Alamos NATIONAL LABORATORY

Our Conclusions

- Layering solid DT in RF foam improves (smoothes) the overall surface roughness 50% or more, by dramatically suppressing mid-mode (10-100) roughness. (The fine foam cell structure causes freezing to begin with the formation of many small, randomly-oriented crystallites, which then propagate into the pure DT solid instead of forming large crystalline facets at the solid-vapor boundary)
- Stepped-ramp cooling of an equilibrated DT solid layer causes surface roughening (from 50-75% using same initial equilibration temperature) that is dominated by mode 2, and modes 10-50 (could re-crystallization be occurring?)
- Re-warming the solid layer smoothes the surface slightly (~15%), but modes 10-50 continue to roughen and dominate (resulting large crystalline facets do not decrease in size?)